# Biophysical and Architectural Mechanisms of Subthalamic Theta under Response Conflict

by

Prannath Moolchand

B.Eng.(Hons.) University of Mauritius, Mauritius, 2010

M.Sc. The University of Sheffield, United Kingdom, 2012

Sc.M. Brown University, United States of America, 2017

A dissertation submitted in partial fulfillment of the
requirements for the Degree of Doctor of Philosophy
in the Department of Neuroscience at Brown University.

Providence, Rhode Island

May 2020

This dissertation by Prannath Moolchand is accepted in its present form
by the Department of Neuroscience as satisfying the
dissertation requirement for the degree of Doctor of Philosophy.

Date 7/16/19 _____
Prof. Michael. J. Frank, Advisor

Date 7/16/19 _____
Assoc. Prof. Stephanie R. Jones, Advisor

Recommended to the Graduate Council

Date 7/14/19 _____
Prof. Barry W. Connors, Reader

Date 7/16/19 _____
Prof. Wael F. Asaad, Reader

Date 7/16/19 _____
Prof. Nancy J. Kopell, Reader

Approved by the Graduate School

Date _____ _____
Prof. Andrew G. Campbell, Dean of the Graduate School

# Prannath Moolchand

*185 Meeting Street, Box GL-N*
*Providence, RI 02912, USA*
✉ *prannath.moolchand@fulbrightmail.org*


## Education

| | |
|---|---|
| | **Brown University**, Providence, RI 02912, United States of America |
| Aug 2012 - Aug 2019 | Ph.D., Neuroscience. |
| Aug 2015 - May 2017 | Sc.M., Applied Math. |
| Aug 2012 - Oct 2014 | Sc.M., Neuroscience. |
| | **The University of Sheffield**, Sheffield, S10 2TN, United Kingdom |
| Sep 2011 - Sep 2012 | M.Sc., Cognitive and Computational Neuroscience, *Distinction*. |
| | **The University of Mauritius**, Reduit, 80837, Mauritius |
| Aug 2006 - Jun 2010 | B.Eng.(Hons), Mechatronics, *First Class with Honours*, ranked first. |

## Fellowship

| | |
|---|---|
| 2017-2018 | Brown Institute for Brain Science Research Graduate Award<br>*Supported by the Dr. Daniel C. Cooper Graduate Award, the Charles A. Dana Graduate Fellowship Fund, and the Department of Psychiatry and Human Behavior*. |
| 2015-2017 | Open Graduate Education, Graduate School, Brown University<br>*Competitive scholarship allowing select Brown doctoral students to pursue a master's degree in a secondary field [Applied Math]*. |
| 2012-2014 | Fulbright Scholarship, US Federal Government<br>*To pursue doctoral studies in Neuroscience at Brown University*. |
| 2011-2012 | State of Mauritius Postgraduate Scholarship, Ministry of Education, Mauritius<br>*Competitive scholarship to pursue master's degree in Cognitive and Computational Neuroscience at Sheffield University - covered all university fees and living stipend*. |
| 2011-2012 | Postgraduate Bursary, Psychology Department, The University of Sheffield. |
| 2006-2010 | University of Mauritius Bursary<br>*Covered all university fees for four-year undergraduate degree, awarded to best candidates ranked at the Cambridge Higher School Certificate International Examinations*. |

## Prize

2010 Gold Medal
*Best Final Year Honours Project in Faculty of Engineering at the University of Mauritius*.

2010 First Prize - Institute of Engineers Mauritius
*Prize money of MUR 25000 awarded for best engineering final year project*.

## Research Experience

2014-2019 Doctoral Dissertation, Brown University

*Biophysical and Architectural Mechanisms of Subthalamic Theta during Response Conflict*

Advisors: Prof. M. J. Frank, Assoc. Prof. S. R. Jones
Doctoral Committee: Prof. B. Connors (Chair), Prof. W. Asaad, Prof. Nancy Kopell (External Reader)

*The need to arrest ongoing or planned actions is a hallmark of adaptive control that is crucial for goal-directed behaviors and survival. When the brain is subjected to competing signals that try to express conflicting behaviors, it needs to halt to evaluate the consequences under volitional control, or to avoid aversive situations through reflexive suppression. The cortico-Basal Ganglia system is responsible for mediating response inhibition to buy the cognitive system time to implement the appropriate action. A subcortical brain area whose dysfunctions result in pathology such as Parkinson's, the Subthalamic Nucleus (STN) is responsible for braking behavioral expression. Experiments have shown that under response conflict conditions, STN spiking and theta power are elevated. Unfortunately, the electrophysiological mechanisms underlying these neural signatures remain poorly understood. To address this, we have built a novel biophysically principled large-scale model of the subthalamopallidal network, including prototypic and arkypallidal units, that is sparsely and probabilistically connected. Conflict was simulated by driving cortical input to STN and varying the level of co-activation across cortical feeds. We test how biophysical, cortical dynamics, and architectural constraints impact the relationship among cortical conflict, STN theta power, and spiking. Our simulations show that the STN-GPe network does not resonate at theta on its own, but can do so in response to cortical theta or to cortical burst-events representing action selection dynamics. Rhythmic burst-events, representing a state of conflict when cortical motor plans vacillate in the theta range, led to prolonged theta and increased spiking, consistent with empirical literature. Analysis of underlying mechanisms revealed that NMDA, but not AMPA, currents were necessary and sufficient for theta power expression and for an empirically observed STN triphasic response characterized by spiking, silence and bursting periods. Finally, theta band resonance was also strongly modulated by architectural constraints, with maximal theta with increased presence of STN "coincidence-detector" units that receive input from multiple cortical populations, due to an NMDA-dependent supralinear response. Our results are insightful in connecting biophysical principles with dynamic and architectural constraints to under-*

*stand the nature of STN processing in response conflict, the disruption of which can lead to impulsivity and compulsivity.*

2011-2012 Master's Thesis, The University of Sheffield

*Micro-circuit models of basal ganglia: Role of peptides in action selection*

Advisors: Prof. K. Gurney, Prof. P. Overton

*Based on novel empirical findings that Substance P (SP), a metabotropic neurotransmitter, can mediate excitatory interactions among Medium Spiny Neurons (MSN) in the striatum, the input of the Basal Ganglia, my project investigated the potential for SP mediated cooperative dynamics among MSNs in the otherwise GABAergic based competitive dynamics in the striatum, and how they may affect action selection. To address this quesiton, I built a microstriatal circuit using Izhikevich based models for the MSNs, and constructed a model for the modulatory effect of SP that captured both SP kinetics and its physiological effects on individual MSN. Our network results showed that SP modulation increased and synchronzied MSN spiking, that could help one action to be selected over another one whose MSNs fire at lower rates and with lower synchrony.*

2009-2010 Undergraduate Honors Thesis, University of Mauritius

*Intelligent System for Collision Avoidance in a Multiple Robot System*

Advisor: Prof. H. C. S. Rughooputh

*I designed an intelligent high level coordinator that analyzed the planned trajectories of two independent robots interacting in a dynamic environment to detect and prevent potential collision by modifying their trajectories. I trained an Artificial Neural Network to do nonlinear mapping between robotic arm positions and joint angles to solve the inverse kinematics problem so that the robot could follow any possible path in a plane whilst minimizing energy and generalizing to unprecedented situations. Using Adaptive Neuro Fuzzy Inference System, the controller could detect collision by analyzing the kinematics, and intelligently decide on modifying trajectories that ensured minimal and smooth deviations from original paths by avoiding abrupt velocity changes. I built the 3D robotic arm models in SolidWorks and interfaced them with MATLAB/Simulink to succesfully demonstrate the ability of the hierarchical coordinator to detect and avoid collisions, without catastrophic failures in the event of new situations.*

## Publications

2019 Biophysical and Architectural Mechanisms of Subthalamic Theta during Response Conflict, pre-submission.

## Teaching Experience

| | |
|---|---|
| 2015 | Teaching Assistant for Computational Neuroscience NEUR1680, an advanced undergraduate course taught by Prof. Elie Bienenstock<br><br>*Held TA hours to assist - both undergraduate and graduate - students with class materials, research papers, projects and coding; Also helped them with building requisite math background, particularly statistics and some fundamentals of dynamics; Graded homeworks and final projects*. |
| 2015-2018 | Undergraduate Mentoring<br><br>*Taught basics of computational neuroscience with particular focus on Hodgkin-Huxley formalism; introduced dynamical systems concepts; taught scientific computing including high performance computing; provided guidance with literature survey, designing and running computational neuroscience experiments, and analysis*. |

## Laboratory Experience

| | |
|---|---|
| 2011- | Biophysically based Neuroscience Modeling (molecular, cellular, network). |
| 2012-2013 | Electrophysiology & Optogenetics in rat/mice hippocampus - slice preparation and patch clamp recording. |
| 2013, Jan | Neuro-practicuum, Marine Biological Labs, Woods Hole, MA. |
| 2006-2010 | Robot Programming, Programmable Intelligent Computer (PIC), Design and implementation of several electrical/electronics/pneumatic/hydraulic systems (projects to solve particular problems)<br>Conducting experiments to test basic principles in various labs: Electrical Power and Machines, Microprocessor, Instrumentation and Control, Electronics, CAD/CAM, Fluid Power and Drives, Thermodynamics, Metrology, Metallurgy, Mechanical Workshop and Machine Tool, Applied Mechanics and Structures. |

## Conference Presentations

| | |
|---|---|
| 2018, Jul 15 | Computational Neuroscience Conference, Seattle, WA. |
| 2017, Nov 13 | Society for Neuroscience Conference, Washington, DC. |
| 2017, Sep 7 | Cognitive Computational Neuroscience Conference, New York, NY. |

## Skills

| | |
|---|---|
| Programming | High Performance Computing, Scientific Computing, Parallel Coding<br>Low Level: Assembly Language - instruction set (mnemonics, machine code - hex, binary), microprocessor architecture<br>High Level: Python, Matlab/Simulink, C, C++, LabView<br>Software development: Linux, Intel compilers, MPI. |
| Typography | LaTex, Open Office, Microsoft Office, Adobe products. |

Language English, French, Hindi, Sanskrit(Elementary), Mauritian Creole.

## Graduate Courses

| | |
|---|---|
| | Mathematics |
| 2014-2017 | Real Function Theory, Probability Theory, Nonlinear Dynamics, Dynamics & Stochastics, Recent Applications of Probability and Statistics, Functional Analysis (audited), Computational Probability and Statistics (Adv. Undergrad)<br>Adv. Undergrad Audited: Topics in Chaotic Dynamics, Abstract Algebra, Real Analysis. |
| | Neuroscience |
| 2012-2013 | Advanced Molecular & Cellular Neurobiology I (electrophysiology) & II (molecular level), Statistical Neuroscience, Neuroanatomy, Advanced Systems Neuroscience, Advanced Cognitive Neuroscience, Cognitive Computational Neuroscience (adv. Undergrad). |
| 2011-2012 | Computational Neuroscience 1 (biophysical modeling, phase plane/bifurcation analysis) & 2 (theoretical models, RL), Fundamentals of Neuroscience. |

## Referees

CONNORS, Barry W., PhD
L. Herbert Ballou University Professor of Neuroscience, Professor of Medical Science, Brown University
185 Meeting Street, Box GL-N, Sidney Frank Hall Room 460
Providence RI 02912-1821
Phone: +1 401-863-2982, Fax: +1 401-863-1074
BC@Brown.edu.

FRANK, Michael J., PhD
Edgar L. Marston Professor of Psychology Cognitive Linguistic & Psychological Sciences, Brown University
190 Thayer St, Box 1821, Metcalf Room 335
Providence RI 02912-1821
Phone: +1 401-863-6872, Fax: +1 401-863-2255
Michael_Frank@Brown.edu.

JONES, Stephanie R., PhD
Associate Professor of Neuroscience, Brown University
164 Angell St, Room 425
Providence RI 02912-1821
Office: +1 401-863-1000, Mobile: +1 617-921-2412
Stephanie_Jones@Brown.edu.

*More referees available upon request*.

**Acknowledgements**

I seize this opportunity to first thank the American people who sustain the Fulbright scholarship, which enabled my doctoral studies, and Brown University for the opportunities to pursue our research interests in addition to providing financial, academic, health, psychological and emotional support. My wholehearted appreciation goes to the Dana and Cooper families for their contributions to my BIBS graduate award, and to the Open Graduate Education program that allowed me to earn the Masters in Applied Math and to have wonderful conversations with Deans Campbell, Ryan and Weber. Without the support of the Neuroscience staff, we would not be able to efficiently concentrate on the science, so a great applause goes to them.

Over my years at Brown, I have had the privilege to be guided by several people across the Neuroscience and Applied Math departments. Very special thanks go to Prof. D. Lipscombe, Prof. C. Moore, Prof. W. Truccolo, Prof. D. Sheinberg, Prof. A. Hart, Prof. J. Sanes, Prof. D. Berson and Prof. C. Aizenman from the Neuroscience department for their affability, time and advice whenever I needed them. My unreseved gratitude goes to Prof. Kauer who personally taught me hippocampal electrophysiology. I remain ever grateful to Prof. Bienenstock and Prof. Ramanan of Applied Math for some very nice discussions and for guiding my graduate mathematical education.

Next, I thank my committee members, Prof. B. Connors, Prof. W. Asaad and my external reader Prof. N. Kopell for their great guidance in steering my research towards successful completion through their questions that always opened some new avenues for more thoughts and deeper comprehension.

Of note, I have sipped several times from the wisdom of Prof. Connors and Prof. Lipscombe, not only for my doctoral work but also for my longer term interests in neuroscience; I am grateful for their insights, time, advice and encouragement.

I thank members of the Frank and Jones labs for the various intellectual exchanges, support and camaraderie, in addition to the postdocs Dr. C. Deister, Dr. S. Lee and Dr. A Hamid who provided good tips and advice. Nonetheless, a very bright undergraduate from Applied Math at Brown, Maxwell Sherman was very instrumental in getting me up to speed with

the coding and computational modeling, more for his belief that led him to inculcate in me a sense of independence to face all academic adversities unflinchingly. Without any doubt, he is the most intelligent person I have encountered at Brown.

Words would never suffice to thank my mentors, Prof. Michael Frank and Assoc. Prof. Stephanie Jones for their supervision, advice, patience and support throughout the long years in graduate school. Many a times, I would meet them not to show results but to report what is not working. Their understanding and compassion through difficult times will always be remembered, as well as their unwavering trust in my abilities and independence. If I could share my two cents of how I hope to emulate them, of Prof. Frank, I have always been impressed of how he remembers the exact details, figures and nuances from various papers for the multifarious projects and people he magically supervises; of Prof. Jones, I have always appreciated how she invests a lot into crafting a very nice talk, with emphasis on the language coherence and delivery. She wins extra thanks for always thinking about us on her travels and bringing us chocolates. Undoubtedly, they are both great course instructors.

My life has always been blessed with the entourage of many wise and strict gurus. While I remain ever indebted to all those who have taught me since childhood across variegated fields, I have very special regard for Mrs. Labutte, my kindergarten teacher, and Mr. Hurnath, one of my primary school teachers, who taught mathematics not by rote, but through logic, a legacy I carry till today. Mr. Ramchurn, my English teacher, music teacher and essentially life coach, holds a very prominent place in my life, and whose guiding principles I try to adopt. I am also very grateful to Prof. Yugal Kishor Mishra of Varanasi, who along with nurturing my Vedic religio-philosophical curiosity, has emphasized that I prioritize my progress in the scientific field, which he reckons as equally sacred from the Brahmanical perspective.

My all-weather friends number many, and I am but the fortunate product of their bright, kind and loyal company. In particular, I would like to thank Tory, Krishna, Yashil, Harsh and Aakash for helping and supporting me through good and difficult times. David Fekna is my first ever friend, and his great influence in both my academic and personal life is appreciated every single day. All my friends are equal, but Dr. Naresh Rughooputh, is

more equal than others. He is a high achieving genius and laureate from Royal College Curepipe, Mauritius, and a more-than-brother. Without his contagious quest for academic perfection, belief and encouragement, I would neither be a Fulbright scholar nor a Doctor today. This success of mine verily belongs to him as well.

Unconditional encouragement, love and support from my family stand me where I am today. My prayers and gratitude go to my late brother-in-law, Khemraj Mutty, who was always kind, loving and encouraging, and to my sister Kamil, who has always been loving and protective. Special thanks are due to my extended family whose support proved a buoy through very difficult times. I would like to express my gratitude to my wife Heema who was understanding, supportive, and even spent sleepless nights to keep me company while I was travailing through difficult neuroscience coding or impossible mathematical theorems and proofs, and for caring for our baby kind of single handedly. The contributions of my mother and father to my life and intellectual heritage are simply priceless. I thank my mother for she has always been a selfless lady sacrificing for even the slightest comfort of her children, and my father, whose brightness and farsightedness have paved the way for our successes in life. This doctoral degree is a tribute to the fruition of their lifelong perseverance.

Piyushakanti, my lovely, beautiful daughter, the very essence of my world. To her, I first owe innumerable apology. I have stolen her rightful share of paternal time and affection to sail through the last phases of doctoral life. Circumstances demanded this great a sacrifice which, stones in heart, we had to give. I thank her now, tomorrow, and forever, in anticipation of her compassionate understanding and forgiveness, as well as for filling life with all joys and wonders and enthusiasm.

# Contents

# List of Tables

# List of Figures

# Chapter 1

# Introduction

## 1.1 Overview

In our everyday lives, we are often confronted with circumstances when we have to choose among competing and even mutually exclusive options. In such situations, the brain is informed of the competing signals that try to engage the final common motor system to initiate movements for us to interact with the outside world. For instance, consider how US citizens would generally cross the road at a pedestrian crossing without traffic lights. They first look to their left for oncoming vehicles closest to the curb they are at, followed by to their right for oncoming traffic in the opposite direction, and then quickly check to their left again. As they have been doing so for years, these motor sequences associated with the goal of crossing the road have been so reinforced that they are automatically implemented whenever required. However, when they travel to the UK where vehicles drive on opposite sides and wish to cross the road there, the Americans are tempted to look to their left first before crossing the road if they are not attentive to their new entourage. To achieve the same goal, but in this different environment, they need to arrest premature expression of the prepotent behavior and adapt the motor sequences, which requires conscious cognitive control, in contrast to passive execution of automated motor activities.

Behavioral expression requires the coordination of the Cortico-Basal Ganglia system. When a motor program needs to be implemented, the motor cortex sends a signal to the Basal Ganglia [BG] which dynamically disinhibits the thalamus to gate the program through the cortico-thalamic loop, Fig. 1.1A. Reinforced actions tend to be gated more quickly and

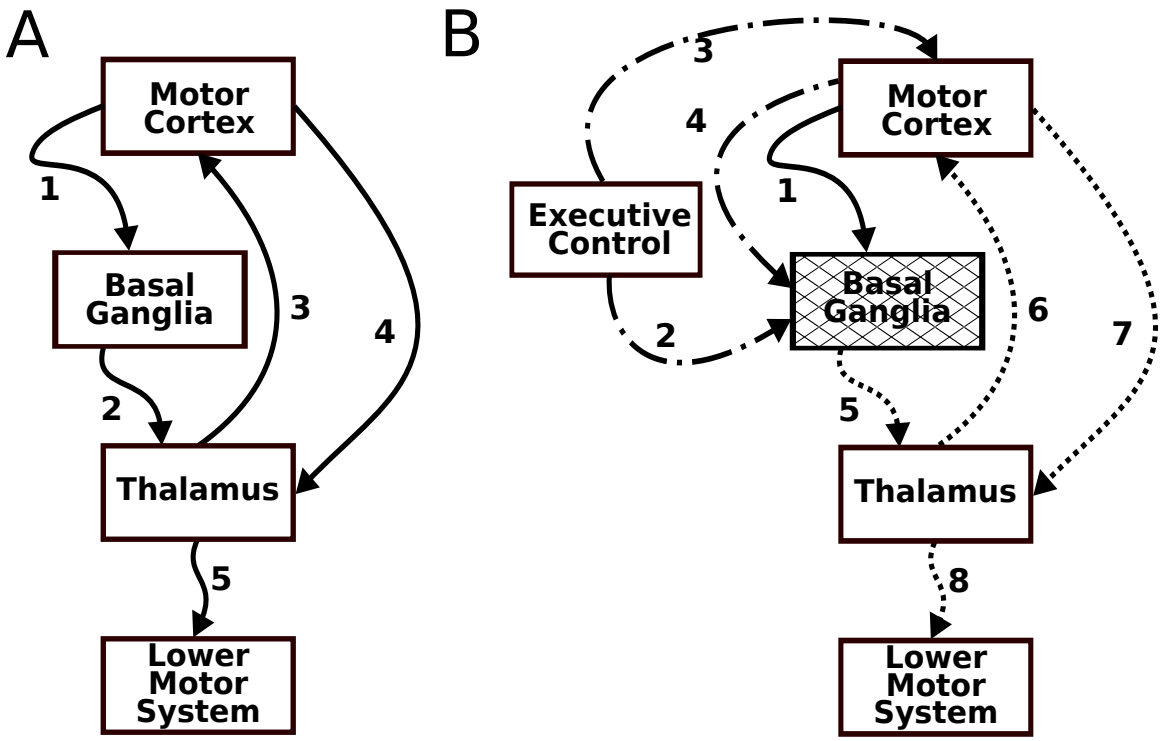


Figure 1.1: **Schematic of the interactions between Basal Ganglia and Corticothalamic loops.** Numbers indicate the sequential stages of signal processing. **A** Under no conflict condition, the Motor Cortex sends a signal to the Basal Ganglia (1) that disinhibits the thalamus (2). This allows the motor program to be gated in the corticothalamic loops (3,4) to access the final lower motor resources(5). **B** When a prepotent activity (1) faces opposition from a mutually exclusive behavior (2), the Executive Control system detects the conflicting signals and participates in braking (3) the BG output to buy the system time to resolve the conflict. Following resolution, the EC communicates the desired motor program (3) to the BG input, and only one of the competing programs (1 or 2) accesses the final motor pathway (5-8) as described in **A**.

easily via the BG. Consequently, when a mutually exclusive action needs to be expressed, voluntarily or involuntarily, we require the Executive Control [EC] system of the Prefrontal Cortex [PFC] to swiftly exert a brake the BG output to halt all behavioral expressions. Arresting such impulsive and potentially inaccurate behaviors buys the EC time to reflect on the more appropriate response and communicate it to the striatum for eventually gating through the cortico-thalamic pathways [1, 2, 3, 4, 5, 6, 7, 8, 9, 10, 11], see Fig. 1.1B.

Simultaneous co-activation of antagonistic neural signals that engage in opposing planned or initiated motor action constitutes a state of response conflict [12, 13, 14]. This state is thought to invoke a dynamic response inhibition mechanism in Cortico-BG circuitry to prevent prepotent responses from being executed prematurely. But what are the dynamical neural mechanisms or correlates of conflict and how are they used to impact behavior?

As the differing tasks engage different cognitive systems and processes, the neural signatures therein are modulated to reflect the various dynamical states across several scales from synaptic activities to spiking to Local Field Potentials [LFP] to electroencephalogram [EEG] signals. One of the main neurophysiological characterization of activities associated with cognitive processes is the spectral representation of recorded neural signals across frequency bands, where both power and phase are studied. The main bands are roughly *delta*, 2-4 Hz, *theta*, 4-8 Hz, *alpha*, 8-15 Hz, *beta*, 15-30 Hz and *gamma*, 30-100 Hz. Combinations of neighboring bands are also studied, such as Low Frequency Oscillation [LFO] band that lumps *delta* and *theta* activities. Of note, theta band activities, with time courses in the range of 125 ms through 250 ms, reflecting 4 to 8 Hz activities, are implicated in various cognitive functions, such as memory and learning [15, 16], facilitation of interregional communication [17, 18], synaptic plasticity [19, 20] as well as behavioral expression [21, 22, 23]. Ubiquitous in the brain, theta band activity is also involved in response control [24], which is a crucial component of conflict resolution [25, 26] in the brain. Unsurprisingly, recent experiments [27, 28, 29] evidence a role for theta band activities during response conflict.

This chapter first reviews the roles of PFC and BG anatomy and physiology in reinforcing prepotent behaviors and how signals opposing them lead to response conflict conditions. The involvement of STN activities via the hyperdirect pathway in inhibiting response is described along with empirical reports that detail the neural signatures and behavioral effects of

disrupting STN function, either physically or physiologically by Deep Brain Stimulation [DBS] or optogenetics. A description of existing models across different levels, such as systems level network model and the drift diffusion model, that capture both the neural signals and the behaviors is provided along with their predictive contributions. Next, I discuss the limitations of current models in explaining the recorded oscillatory signals, and how that motivates the need for a biophysical model with a physiologically relevant timescale to capture the temporal aspect precisely. This chapter concludes with the open questions that are addressed in this doctoral work.

## 1.2 The Cortico-Basal Ganglia system in Prepotent Behavioral Expression and Response Inhibition

### 1.2.1 The Cortico-Basal Ganglia system facilitates behavioral expression through action selection

The Basal Ganglia are a set of subcortical nuclei that have been implicated in both motor and cognitive functions. Conserved across vertebrates, it is estimated to be at least 400 million years old [9]. One of its major functions is action selection, achieved by facilitating the execution of a single motor program while suppressing the competing ones [10, 11, 30, 8, 31, 32].

As shown in Fig. 1.2, the BG consists of three main pathways. Briefly, the input nucleus of the BG is the striatum that receives dense cortical innervations. The output nuclei are the Globus Pallidus internus and the Substantia Nigra pars reticulata.

The direct (GO) pathway, involved in facilitating actions and sensitive to reward, features a direct connection from the input to the output nuclei, while the indirect (NoGo) pathway, involved in suppressing actions and sensitive to punishment, features an intermediate station known as the Globus Pallidus externus between the input and output nuclei [7, 1, 8, 9, 10, 11]. An action is eventually selected based on the activities in these two pathways [32, 3, 4, 5, 2, 6], as described below. The STN is the only excitatory nucleus releasing glutamate in this otherwise GABAergic circuit, and innervates both portions of the Globus Pallidus,

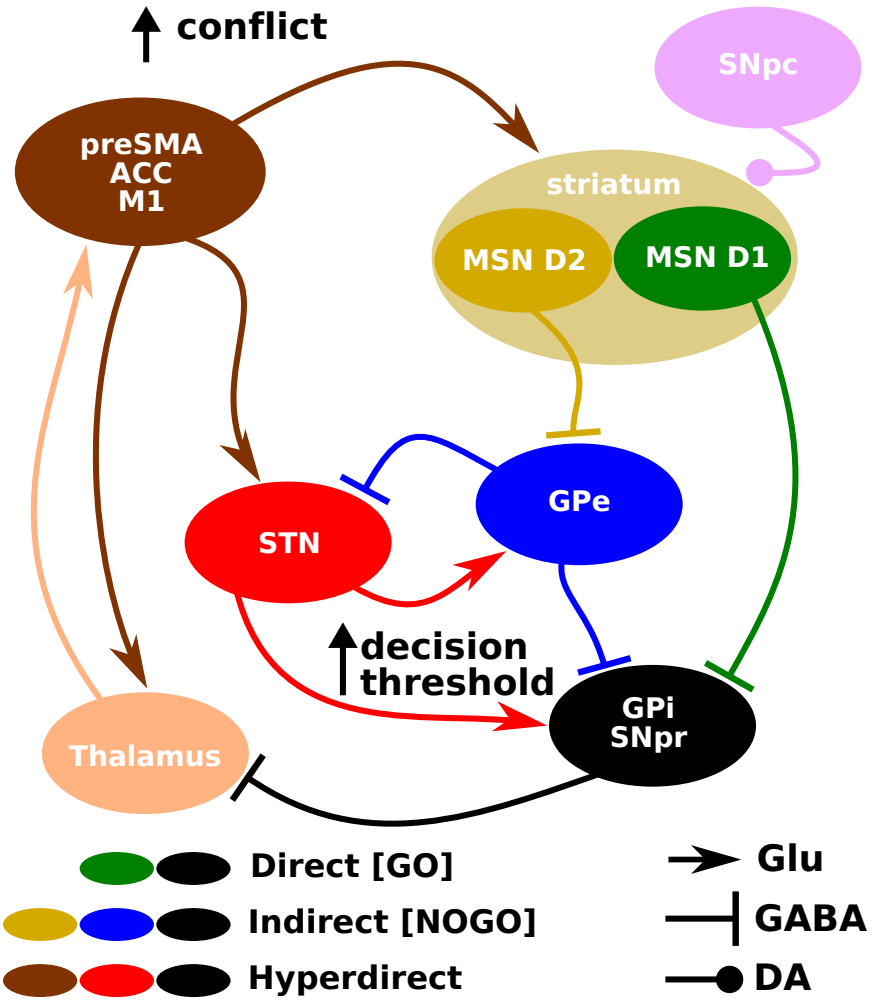


Figure 1.2: **Schematic of the Basal Ganglia circuitry.** Line ends represent neurotransmitter release; Glu: Gluatamate (Excitatory), GABA: Gamma-AminoButyric Acid (Inhibitory), DA: Dopamine (Modulatory). It consists of three main pathways, the Direct (GO), the Indirect (NOGO) and Hyperdirect direct. The striatum contains two subpopulations of Medium Spiny Neurons (MSN) that express either D1 or D2 dopamine receptor channels. The striatopallidal pathway starting with the D1 MSNs innervating the Substantia Nigra pars reticulata (SNpr) and Globus Pallidus internus (GPi) is termed the Direct pathway. It is involved in learning and facilitating rewarding actions. The Indirect pathway starts with the D2 MSNs and innervates the SNpr and GPi via an intermediate station, the Globus Pallidus externus (GPe). It is more involved in learning aversive outcomes and preventing them. The cortico-subthalamic pathway, also known as the Hyperdirect pathway, connects several parts of the cortex to the subthalamic nucleus that innervates the SNpr and GPi. It allows the cortex to exercise control on the output of the Basal Ganglia. Moreover, the Subthalamic Nucleus and the Globus Pallidus externus share reciprocal connections, STN exciting GPe that inhibits it back. Functionally, when conflict level increases in the cortex, the STN is excited and raises the decision threshold to prevent any actions gating through the GPi/SNpr.

namely the GP externus and GP internus, and the Substantia Nigra pars reticulum [SNpr] while it receives reciprocal inhibition from the GPe. While the classical model comprising the two striatopallidal pathways and the subthalamopallidal loops was useful for accounting for a variety of data, the more recent discovery of the hyperdirect pathway that provides direct monosynaptic connections from the cortex to the STN [33, 34, 35, 36, 1] prompted a revised understanding of the cortico-BG system. Ensuing theoretical and empirical research has shown that cortically driven STN activity – particularly during response conflict or surprising situations – plays a crucial role in response inhibition [37, 38, 39, 40, 41, 29, 42, 27, 43, 44, 45, 46, 47, 48] by exciting the SNpr/GPi to enhance inhibition of the thalamus and thus prevent motor expression via the thalamocortical loops, Fig. 1.2. In so doing, the STN overrides the striatopallidal control over motor behavior and provides a quick mechanism for cortex to influence behavioral expression. Halting the BG output is a crucial ingredient in adaptive control for goal-directed behaviors under volition and for survival by reflexively suppressing aversive actions in more involuntary circumstances.

### 1.2.2 Prepotent action selection results from dopaminergic Reinforcement Learning

Action selection through the BG is a dynamic process. Figures 1.1 and 1.2 depict the circuits and pathways mediating this process. When an action is presented at the striatum, its levels of reward and penalty are respectively weighed along the Direct and Indirect pathways, with action selection and inhibition as the respective consequence of this tug of war.

The striatum consists of Medium Spiny Neurons (MSN) that express either D1 or D2 dopamine receptor channels. The MSN subpopulations expressing D1 and D2 receptor channels form the starting point of the Direct and Indirect pathways respectively. When the D1 receptor is activated, it has a net excitatory effect on the cell, while its D2 counterpart has a net inhibitory effect. The striatum receives a basal level of dopamine from the Substantia Nigra pars compacta, which sets the basal levels of activities in both pathways.

During reinforcement learning, when a novel rewarding action is selected, there is a burst in activity in the dopaminergic cells [49], while a dip is observed when the action turns out to

be aversive. These differing levels of dopamine release in the striatum drive corticostriatal plasticity, with the burst promoting plasticity in the direct pathway to code for rewarding values while the dip doing likewise in the indirect pathway to code for penalty values.
Hence, the synaptic strengths of the cortico-striatal connections inform the relative reward versus penalty values, based on past reinforcements. Moreover, based on reinforcement only, when two rewarding or two aversive actions compete with each other, the one with the higher reward versus penalty value tends to get selected.
In the context of our example, the motor sequences of left-right-left have precedence when the goal is to cross the road. However, when the person needs to cross the road in the UK, the brain has to quickly take cognizance of the different environment, and the behavior should be accordingly updated, namely to a right-left-right sequence. This, however, constitutes a conflict situation as looking to the left first is the prepotent activity while looking to the right is the required one. Moreover, the brain must be able to quickly halt execution of such potentially harmful motor programs that would otherwise be preferentially selected based on reinforcement.

### 1.2.3 Response Inhibition Mechanism is critical for arresting prepotent motor response

Response Inhibition is a critical component of motor control and its timely implementation can be the difference between death and survival. It is employed both in consciously withholding motor expression and reflexively withdrawing from premature motor output in response to external stimuli that may signal danger. Contextually, crossing the road in the different environment may engage the response inhibition mechanism by both reflective and reflexive action [50, 37, 51]. For instance, in the former case, an attentive person may realize the realize the different setting and elects to proactively restricts the prepotent urge to look first to the left. Alternatively, an inattentive person may not implement volitional control whereby the prepotent activities involuntarily get initiated. However, if the person is informed of impending danger such as a honk or a road sign that instructs to look to the right, the response inhibition mechanism is triggered and the person may arrest the behavior. The earlier the initiation of the antagonistic signal, the more likely the response

inhibition is successful.

Several brain areas have been implicated in response inhibition, namely the Inferior Frontal Gyrus (IFG), the pre-Supplementary Motor Area (preSMA) and the STN [52, 27, 53, 37]. Since the IFG and the preSMA, respectively parts of the Executive Control and Motor Implementation systems, directly innervate the STN which can monosynaptically influence BG output, the latter stands in a good position to implement the required braking mechanism whilst integrating cortical information.

### Cortical drive to the Subthalamic Nucleus via the Hyperdirect pathway brakes Basal Ganglia output

Modifying the behavior takes time, while the previously reinforced rewarding movements are primed for execution. Therefore, we have to be capable of quickly halting the latter activity to buy the system time to eventually decide on which actions lead to the goal in the different environment. Based on the physiologies of the different BG pathways, the hyperdirect one has been implicated in such function [33, 38, 39, 40, 41, 29, 42, 27, 44, 45, 46, 47, 48]. Cortical excitation of the STN causes a phasic increase in firing rates of the GPi and SNpr to further inhibit the thalamus. Therefore, any action that seeks to gate through via the GO striatopallidal projections need to overcome the STN mediated enhanced inhibitory effect of the GPi and SNpr in order to disinhibit the thalamus. In sum, it can be construed that the STN brakes the output of the BG by eventually raising the threshold such that no action can be selected (see Fig. 1.2).

In a situation of conflict when two mutually exclusive actions try to access the final motor resources, the BG is faced with an over-constrained system that it cannot accurately solve. However, because it is the motor cortex that presents competing signals to the striatum, conflict should first be solved in higher motor areas such as the Anterior Cingulate Cortex and pre-Supplementary Motor Area, and communicated to the lower level primary motor cortex. The brain relies on the Executive Control system to resolve which signal eventually excites the striatum to request gating. The frontal cortex thus not only has to swiftly direct the STN to halt implementation of BG outputs, but also needs to resolve the conflict. The sequential interactions are summarized in Fig. 1.1.

## 1.3 Empirical Literature on Effects of disrupting STN activity on response and its neural signatures during Response Conflict

### 1.3.1 Disrupting STN activity affects reaction times and response accuracy

STN activities are disturbed in two main ways, namely physically through subthalamotopy or excitotoxic lesions, and physiologically through Deep Brain Stimulation (DBS) or pharmacological blockades.

#### Physically disrupting STN activity

Baunez, Nieoullon, and Amalric [54] induced striatal DA depletion in rats and observed motor initiation deficits, delayed responses and longer reaction times in a reinforcement learning task. Bilateral excitotoxic lesions of the STN reversed the motor initiation deficits, and promoted premature responses with shortened reaction times. The results indicated that the STN played a crucial role in controlling behavioral expression.

In another set of experiments using a five-choice paradigm, Baunez and Robbins [44] showed that bilateral STN lesions in the rats impaired their discriminative accuracy, and caused compulsive behaviors in addition to elevated premature responses, thus establishing the necessity of proper STN functioning in restraining inappropriate motor actions. Further experiments [45] confirmed these observations.

#### Physiologically disrupting STN activity

Frank, Samanta, Moustafa, and Sherman [55] subjected PD patients, with implanted DBS electrodes in the STN, to a probabilistic learning task which manipulated the conflict level under which the patients had to respond. They showed that DBS stimulation caused the patients to respond impulsively with shorter reaction times [RT] and higher proportion of errors. These findings confirmed the predictions of a computational model [38] that interfering with normal STN function by DBS compromises its basal level of braking with

the lesser restraint on motor activities accounting for impulsive behaviors.

Using a Simon task, Wylie, Ridderinkhof, Elias, Frysinger, Bashore, Downs, Wouwe, and Wildenberg [56] similarly disrupted STN activities through DBS stimulations in PD patients, and found that they caused marked impulsive responding with shorter RTs and lower accuracy for incongruent trials. This again highlighted the need for proper STN function to pause responding to buy the executive system time to resolve conflict and implement the correct responses. More recently, Ghahremani, Aron, Udupa, Saha, Reddy, Hutchison, Kalia, Hodaie, Lozano, and Chen [57] used DBS to disrupt STN function tied to specific phases during a Stroop task and confirmed a direct causal role for the STN in assisting conflict-related processing.

To test how the STN is involved while the executive system integrates information from disparate stimuli before responding, Coulthard, Bogacz, Javed, Mooney, Murphy, Keeley, and Whone [58] presented a triad of consecutive stimuli, each a presentation of two symbols to guide response [55], and similarly used DBS to disrupt STN activities. They found that when the first two stimuli would lead to consistent responses, thus making the latter prepotent, while the third indicated an alternative conflicting response, DBS stimulation caused the patients to respond impulsively in choosing the incorrect prepotent action. In addition to its mechanistic braking activities, the STN serves a more fundamental role in enabling complex cognitive functions.

Similar experiments [59] were carried out to investigate the influence of STN on the speed-accuracy trade-off under a moving dot coherence task. They found that patients under DBS stimulations were less likely to pay heed to the instructions and their responses accorded more with their prepotent tendencies. They also reported that the effect of instruction mattered less in low conflict for higher accuracy in contrast to high conflict where the success of the trial was tied with attending to the instructions.

More recently, Fife, Gutierrez-Reed, Zell, Bailly, Lewis, Aron, and Hnasko [52] have shown that optogenetically stimulating the STN caused mice to interrupt their behaviors. Since surprise is a natural cause for suppressing ongoing activities, they also inhibited the STN and found that the ability to pause in response to surprise is diminished, thus revealing a causal role for the STN in arresting behaviors under cognitive demands.

Both structural [54, 44, 45] and functional [55, 56, 58, 59, 52] disruptions of the STN have shown its importance in response inhibition which is an indispensable process in conflict resolution. Interfering with the normal functioning of the STN, such as by DBS, compromises its ability to brake the BG output. This leads to impulsive reactions that are more often erroneous as the system does not get enough time to assess and evaluate competing, hence conflicting, responses. Having established the importance of the STN in conflict condition, we now investigate the nature of STN responses and its interaction with the cortex along the hyperdirect pathway under conflict condition.

### 1.3.2 STN spiking increases upon successful inhibition

Isoda and Hikosaka [40] subjected two monkeys to a Switch-Trial-Task while recording in the STN. After fixation, they were presented with two squares of different colors as stimuli on opposite sides of the screen. For a correct response, the animals had to saccade to the stimulus that matched the color of the presented cue. By successive presentation of the same cue, the animals saccading responses were primed by having faster RTs. To induce conflict condition against such prepotent behaviors, the cue's color was changed in switch trials. Under successful switches, the monkeys had slower RTs while STN spiking increased, Fig. 1.4 A,B. Conversely, faster RTs and no increase in STN activities were noted for failure to make the correct switch. Thus, STN spiking is important for arresting impulsive behaviors. Similarly, Schmidt, Leventhal, Mallet, Chen, and Berke [42] subjected rats to a Stop-Trial-Task where they recorded extracellular STN activities. They showed that increased STN spiking is necessary for arresting Cue-triggered planned movement in response to the Stop cue. They categorized the Go trials into Fast Go and Slow Go and showed that the time courses of STN activities for failure to stop resembled the Fast Go, while Slow Go aligned more with those associated with successful stop.

Zaghloul, Weidemann, Lega, Jaggi, Baltuch, and Kahana [41] recorded from 14 PD patients undergoing DBS surgery, collecting activities from 18 microelectrodes in the STN while they performed a probabilistic learning and decision making task, similar to the one in Frank, Samanta, Moustafa, and Sherman [55], that tested for different levels of conflict. They pooled the spiking activities of the STN cells they recorded from, and showed that during

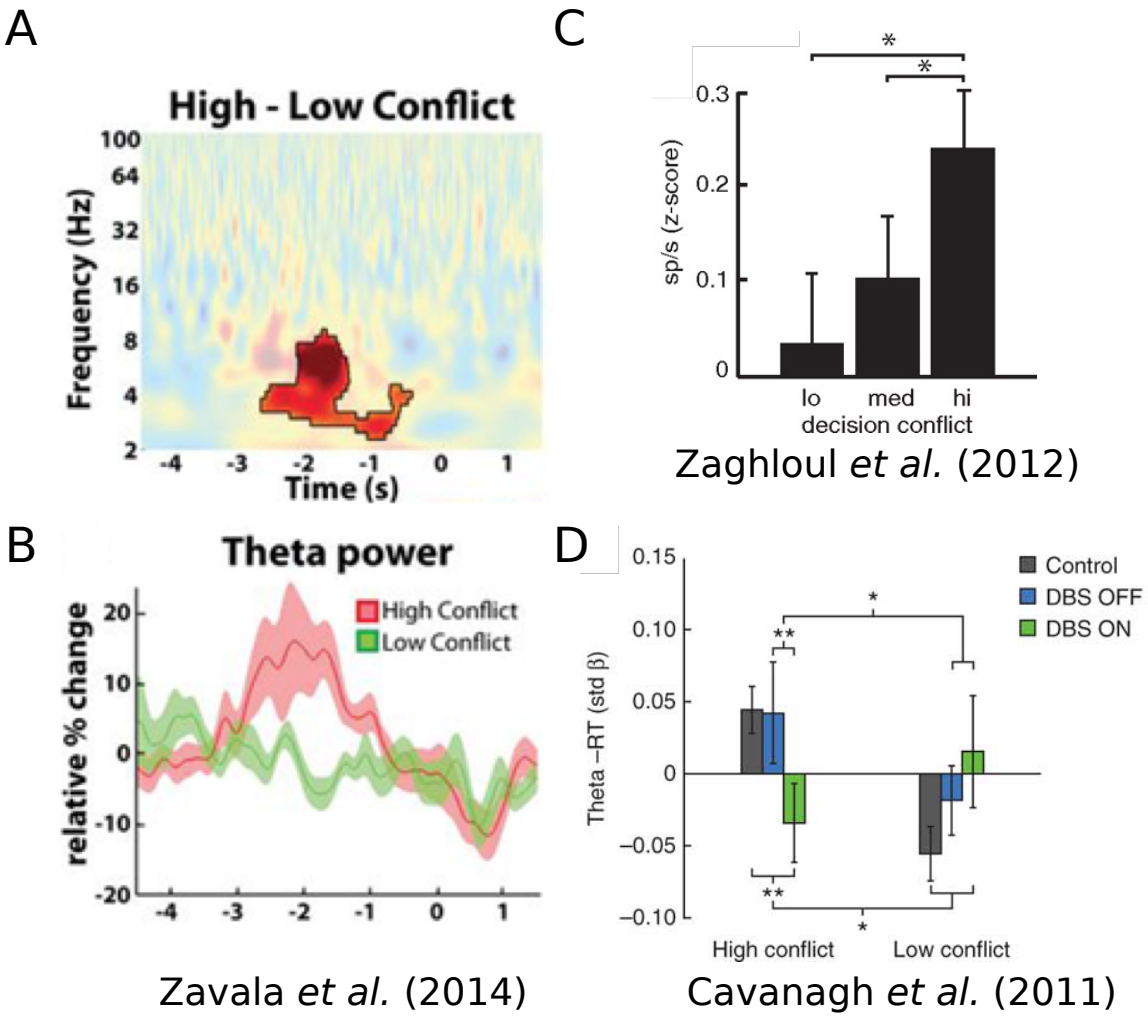


Figure 1.3: **Neural signatures of conflict in the STN.** STN theta power **A, B** [29] and spiking **C** [41] increased with higher levels of conflict when PD patients were subjected to a probabilistic learning task [PLT] where they had to choose between two visual cues that coded for different reward probabilities. **D** Under High conflict condition, higher theta in the medial PreFrontal Cortex correlated with longer reaction times [RTs] [27], whereas it predicted lower RTs under Low Conflict when PD patients performed a PLT. DBS stimulation of the STN reversed the correlations between theta and RT.

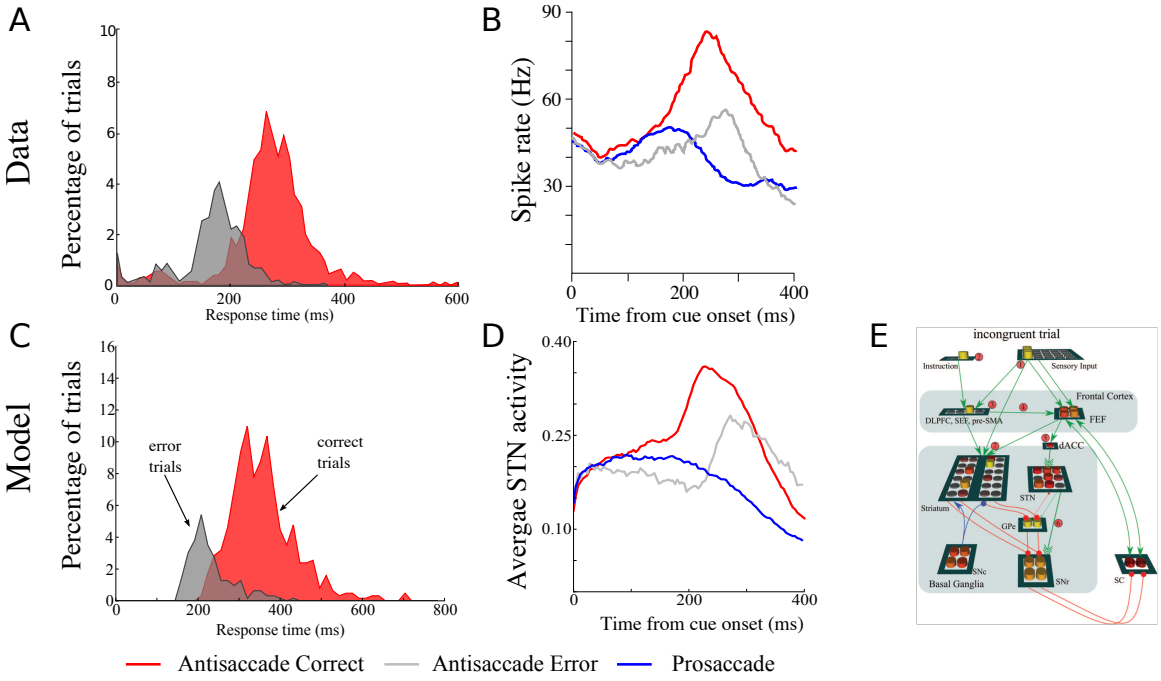


Figure 1.4: **Systems level model captures behavioral data through mPFC-STN interactions. A,B** Monkey data [40]. **C,D,E** Model data [14]. **A,C** Distributions of reaction times for correct (red) and (incorrect) switch trials are longer and shorter respectively. **B,D** STN activities increase in successful switch trial (red) to suppress primed behavior, while failure to elevate activities leads to erroneous response (gray). **E** Systems level (Emergent model) interactions among various nuclei of the cortex and BG are required for the STN to suppress planned activities in a diffuse global NoGo manner.

high conflict, the STN neurons had higher firing rates than during low conflict condition , Fig. 1.3C. In sum, the dynamic alterations in spiking rates of STN neurons for correct responses during conflict are consistent in both non-human and human primates.

### 1.3.3 Systems level modeling predicted that STN braking is implemented via a Global NoGo mechanism

While Aron, Behrens, Smith, Frank, and Poldrack [37] indicated the regions involved in response inhibition and Isoda and Hikosaka [40] showed the STN spiking patterns associated with both successful and unsuccessful response inhibition and task accuracy, the relationship between the observed behavioral measures of reaction times and the cortico-basal ganglia circuitry to account for them was not clearly understood. To address this lacunae, Wiecki and Frank [14] built a systems level model, Fig. 1.4E, comprising nuclei of Frontal Cortex

and BG as well as sensory inputs to investigate the interactions among various areas that could capture the electrophysiology and behavioral observations. They tested the network across many tasks, including the Switch Trial Task, and were successful in replicating the reaction time distributions and STN activities, Fig. 1.4C,D , under both 'Successful Switch', 'Unsuccessful Switch' and 'Non-Switch' trails observed by Isoda and Hikosaka [40].

They found that response inhibition necessitated the STN to excite the output of the BG to inhibit action selection in a global NoGo manner, Fig. 1.5A, that is, once conflict related braking machinery was engaged, it did not filter which motor programs to locally inhibit, but rather did so at a more general level. This is akin to the STN dynamically setting a higher decision threshold such that any action trying to gate through the basal ganglia, along the GABAergic striato-nigral pathway, would consequently need to provide more inhibitory postsynaptic currents to offset the STN's excitation that prevents disinhibition of the thalamus.

The behavior of the network model could be approximated by quantitative fitting with the Drift Diffusion Model [60], Fig. 1.5B, that captures how STN manipulations dynamically affect the decision thresholds to explain the distributions of reaction times for both accurate and inaccurate responses. When STN activity is high, the decision threshold is high and it takes longer to hit the barrier. That reduces the probability that initial evidential accumulation towards a wrong decision will eventually cross the threshold to be selected. On the other hand, a low decision threshold, tied to low STN activity, would allow a greater proportion of wrong decisions to be made, and with lower reaction times, as empirically observed in [55, 27] where impulsive responses showed less accuracy.

### 1.3.4 Decision Thresholds are related to Theta Band activities

Cavanagh, Wiecki, Cohen, Figueroa, Samanta, Sherman, and Frank [27] subjected PD patients to the Probabilistic Learning Task [55] whilst recording activity over the medial PreFrontal Cortex using scalp EEG electrodes. When the patients were under the state of uncertainty which increased with the experimentally induced level of conflict, spectral analysis of EEG signals over the mPFC revealed resonance of theta band [4-8 Hz] power. Disrupting STN activity via DBS stimulation perturbed the mPFC theta signals.

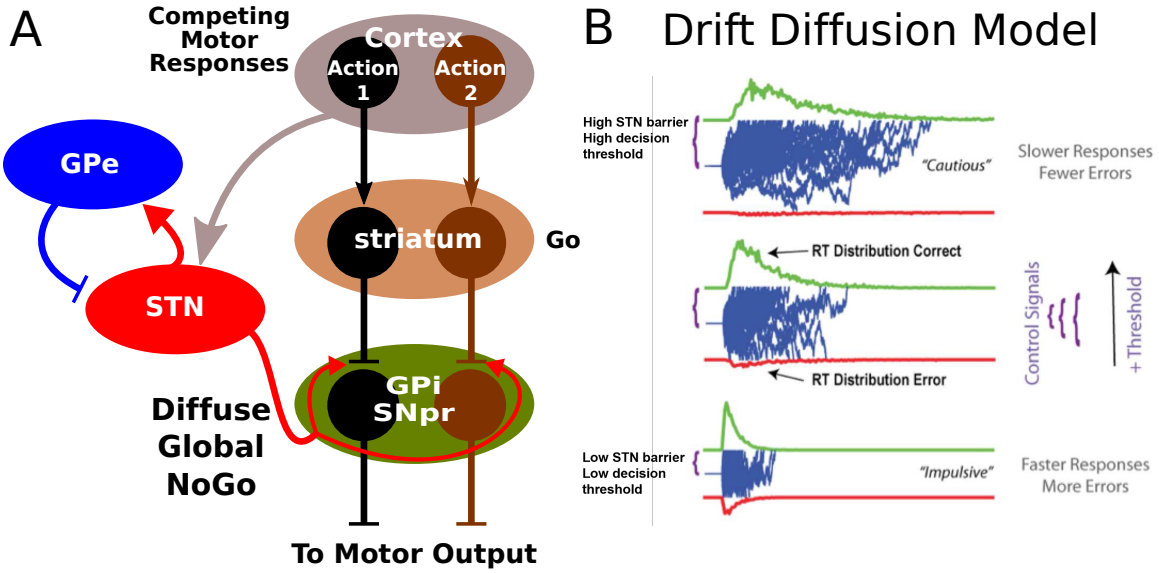


Figure 1.5: **STN global NoGo mechanism and the Drift Diffusion Model. A** When two competing motor actions are considered in cortex, they excite the striatum, the input of the Basal Ganglia, to inhibit the BG output, GPi and SNpr, via the Go pathway to access lower motor resources. See Fig. 1.1 for more details, including activities of GPe in the NoGo pathway. The STN concomitantly receives the excitatory signals for the cortex via the hyperdirect pathway, and subsequently excites the GPi/SNpr in a diffuse global NoGo manner to brake the gating process, thus halting *all* actions from gating through. By so doing, the STN dynamically sets a high decision threshold. **B** The Drift Diffusion Model is a stochastic model that captures the effects of STN activities, decision thresholds, reaction times and accuracy, see also Fig. 1.4. Briefly, when the STN activity is high, it dynamically sets a high decision threshold so that it takes longer to hit the barrier, but with gain in higher proportions of correct responses (green) and reduction for incorrect responses (red). With a lower barrier, it takes less time to hit the barrier but at the cost of lowered accuracy, that is typical of impulsive behaviors.

This line of work motivated further work in patients to understand the neural signatures of decision threshold in the STN.

### 1.3.5 STN theta power increases with conflict levels

In another conflict task, Zavala, Tan, Little, Ashkan, Hariz, Foltynie, Zrinzo, Zaghloul, and Brown [29] recorded LFP signals from 13 PD patients undergoing bilateral electrode implantation in the STN during DBS surgery, and scalp EEG over the mPFC. They thereafter participated in a moving dot tasks that could simulate different levels of conflict. Briefly, when the ratio of dots moving in one direction to those moving in the opposite direction is high, it constitutes a low conflict case, whereas a ratio nearing one represents high conflict. Their spectral analyses not only revealed that theta band activities were modulated under high conflict, Fig. 1.3 A, B, but they also showed that the theta signal in the mPFC was Granger causal to the theta in the STN, suggesting that mPFC theta was driving STN theta.

#### Theta and Reaction Time correlations differ between Low and High conflict conditions

The above studies [27, 29] have established a role for theta band oscillations both in the STN and midline frontal cortex. Interregional communication [17, 18] is also subserved within the theta range. Integrating these two facts suggests that the cortico-subthalamic communication in the hyperdirect pathway may be in the theta range that relays some specific information from prefrontral cortex to STN.

However, Cavanagh, Wiecki, Cohen, Figueroa, Samanta, Sherman, and Frank [27] showed, Fig. 1.3D, that theta band power increase correlated with increase in reaction times only under the high-conflict condition in healthy controls and OFF DBS patients. The trend was reversed with DBS ON. In the low-conflict condition, the relationships between theta power increases and reaction times were negative for both healthy controls and OFF DBS patients. Likewise, DBS caused an inverse relationship. This directly shows that mPFC theta may not be a hallmark of conflict *per se*.

Likening the fact that correct trials required longer reaction times for the high conflict

condition than for the low conflict [55, 59]) to the fact that higher theta power was observed in the high conflict condition in the STN [28, 29], it follows that STN theta band power correlates positively with increase in reaction times.

If cortical theta was a measure of conflict, we would expect it to have a positive correlation with reaction time even in the low conflict case, albeit a smaller one as compared to the high conflict case. Moreover, Zavala, Tan, Little, Ashkan, Hariz, Foltynie, Zrinzo, Zaghloul, and Brown [29] showed that under low conflict condition, cortical theta is not Granger causal to STN theta, while the reverse holds true for the high conflict case.

This suggests that the communication between medial prefrontal cortex and STN via theta band power modulation may not be conveying information about the level of conflict that correlates positively with reaction time. Given the above, we propose that STN may not just be mechanistically applying the brake on the BG under the dictate of the cortex to halt behavior, but rather the STN may be participating at a more cognitive level during conflict condition.

Further work from Herz, Zavala, Bogacz, and Brown [48] showed a similar trend in STN theta power, and they argued that the relationship between STN theta and decision threshold, equivalent with reaction time, could be attributed to the level of cautiousness. Under High Conflict conditions, higher levels of cautiousness are reflected in higher theta power and longer reaction times. Likewise, low level of cautiousness accompanies lower theta power.

## 1.4 Implications for cortico-STN conflict signaling

### 1.4.1 A role for the Subthalamic Nucleus as a conflict detector

Conflict processing involves two main stages, namely conflict detection and conflict resolution. Several lines of evidence implicate the Anterior Cingulate Cortex (ACC) [61, 62, 63] in conflict detection while dorso lateral prefrontal cortex, part of the Executive Control system (see Fig. 1.1), is mostly involved in conflict resolution [64, 63] when the STN brakes the output.

Because detection and resolution are dissociable stages, the former more bottom-up and the

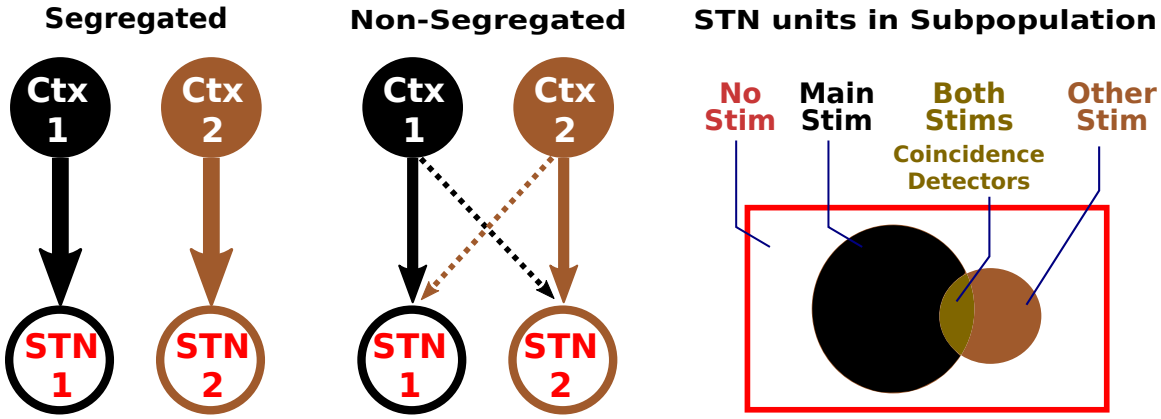


Figure 1.6: **Cortico-STN topography** Subpopulations of the STN receive efferent copies of motor signals that try to access lower motor neurons via the Basal Ganglia for behavioral expressions. Co-activation of several STN subpopulations from different cortical subpopulations makes the nucleus more excitable, and thus the STN itself acts as a conflict detector and brakes the Basal Ganglia output to prevent gating of any of the competing corticothalamic signals. *Left:* In a segregated topography, the cortical information about a particular motor program is sent to one subpopulation only, implying that information is segregated through an organized columnar architecture. *Middle:* In a non-segregated scheme, cortical information is also shared with STN subpopulations that code for competing motor programs. Such a network is characterized by more disperse connectivities between the cortex and the STN. The more the synaptic dispersion, the less the segregation of information. *Right:* The non-segregated network gives rise to four distinct classes of STN units in any one subpopulation by virtue of how they are cortically driven, in contrast to the segregated case where all STN units listen to a single cortical program. Since the cortico-STN topography is probabilistically implemented in the non-segregated case, some units may receive no inputs, the majority receive from the motor program the STN subpopulation essentially codes for, some receive from other single cortical programs only and some will receive from more than one single motor program. The latter act as coincidence detectors, and the lower the segregation level, the greater the proportion of coincidence detectors units in the network
.

latter more top-down in their signaling, conflict detection can be initiated at a lower level in the motor hierarchy. As regards conflict detection, it may be initiated in the cortex and be communicated to all the STN neurons via the hyperdirect pathway. Under the dictate of the frontal cortex, the STN neurons thus mechanically apply the brakes to halt any motor programs, as per Fig. 1.6.

Alternatively, via the hyperdirect pathway, the STN may be informed of the different competing motor programs that seek gating via the BG [55]. This demands that it receives efferent copies of motor programs, and this is supported by the fact that its cortical afferents derive mainly from axon collaterals of cortico-fugal pyramidal-tract neurons [65, 33,

66] that are essentially involved in transmitting motor commands.

In such a topographical organization, (Fig. 1.6, left) distinct subpopulations of the STN receive distinct motor programs. Indeed, such a somatotopic architecture [67] within the motor domain [68, 69, 70, 71, 72] has been reported. However, the levels of intercommunication among domains and within somatotopic areas remain poorly understood. All these excitatory disparate signals from the STN subpopulations are integrated in the nucleus, and the STN universally applies the brakes to raise the decision threshold to prevent any one motor program gating through. This buys the conflict resolution center time to evaluate the best behavior and to change the cortico-striatal facilitation and inhibition.

The prediction of this model is that under high conflict condition, the dynamic surge in activity, such as increased in spiking rates will be higher, because actions that are trying to gate through more forcefully with higher prepotency will confer higher excitation onto the STN subpopulations. This is summarized in Fig. 1.6. Lower levels of conflict will cause lower net activation of the nucleus, implying a short duration of braking commensurate with a shorter reaction time. We expect that the activities in the different subpopulations will summate to LFPs in the theta band activities.

**Summary**

In sum, experiments have shown that STN is necessary for response inhibition, by globally braking the BG output to pause action selection, thus buying the Executive Control system time to resolve the conflict and implement the desired motor response. STN spiking goes up with the level of conflict and correlates positively with reaction times. The STN dynamically sets a decision threshold so that premature activation of motor signals cannot gate through the BG quickly, thus improving accuracy at the cost of slower reaction times. Decision thresholds have been shown to correlate with theta band power.

## 1.5 Open Questions addressed in this doctoral project

Despite the extensive work in STN electrophysiology and modeling, largely motivated by its involvement in the etiology of PD, the electrophysiological mechanisms by which theta

band power is modulated under response conflict have not been studied. The primary aim of this collaborative efforts between two labs is to fill this lacuna.

### 1.5.1 Electrophysiological basis of theta band power modulation in the STN

Given that neural communication is essentially discontinuous in addition to be highly non-linear, it is not trivial that since the presynaptic structure mPFC shows theta band power during response conflict and that it is Granger causal to STN theta that the latter should directly show theta power. First, LFP power reflects small local circuits activities whereas neuronal communication occurs through synchrony of individual cortical cells firing and leading to neurotransmitter exocytosis to generate an appreciable postsynaptic current to affect the receiving cell.

Moreover, given the tight coupling between the STN and the GPe, it is insufficient to study the STN in isolation. Thus, understanding the mechanisms of theta band power modulation requires a thorough analysis of the main currents in the STN and the GPe cells in addition to their interactions in the subthalamopallidal network, and the latter's response to cortical stimuli.

Several models of STN-GPe network have been built [73, 74, 75], but most of them have not implemented biophysical constraints that have been known in the literature for long [76, 77, 36, 78]. Moreover, several lines of work [79, 80, 81, 82, 83, 84, 85, 86] have pointed to the different physiologies and connectivities of GPe subpopulations, but more often than not, GPe tends to be modeled as a homogeneous population. The resultant network dynamics of these diverse GPe cells need to be explored.

Furthermore, the study of frequency band activities is directly tied to some underlying time course, and this requires a model whose parameters have direct biological relevance, such as the Hodgkin-Huxley formulation. While previously the computational complexity disfavored the extensive use of the latter model, contemporary advances in computational prowess have helped to immensely filled these shortcomings.

### 1.5.2 The effects of cortico-subthalamic topography to facilitate the STN to act as a conflict detector

First, conflict levels and reaction times for accurate responses are positively correlated [41, 55, 40, 14, 42]. If mPFC theta encoded the level of conflict, then irrespective of whether it was Low or High Conflict, this demands that the relationship between mPFC theta and reaction times be positive since reaction times are always positively correlated with conflict levels. However, since this differs between Low and High conflict, this means that mPFC theta *per se* may not be signaling the level of conflict to the STN.

Since STN dynamically raises the decision threshold commensurate with the level of conflict, and given the positive relationship with reaction times even under Low Conflict, this broaches the question as to how the STN is made aware of the level of conflict since the Granger causal mPFC theta appears unable to communicate this.

One possible way for the STN to brake in relation to conflict level to affect reaction times is for the STN to act as a conflict detector itself by exploiting the direct connections between the motor cortex and itself to integrate motor information to raise its own levels of activity.

#### Summary

Integrating across several levels of neuroscience, this doctoral work uses a mechanism-mining approach to firstly understand and provide an electrophysiological account of theta band power modulation in the STN and secondly investigates how the cortico-STN topography can endow it with the ability to serve the systems level function of response conflict detection, a major component of the grander cognitive task of decision making.

# Chapter 2

# Biophysical and Architectural Mechanisms of Subthalamic Theta under Response Conflict

## 2.1 Introduction

Various studies have implicated the Cortico-Subthalamic system via the hyperdirect pathway in successful response inhibition. The subthalamic nucleus [STN] is involved in both the outright need to cancel a planned behavior and in dynamically modulating the threshold in decision making in the face of conflict or uncertainty, leading to slower but more accurate choices [33, 38, 39, 40, 41, 29, 42, 27, 44, 45, 46, 47, 48, 50, 37]. The STN mediates these functions by exerting a brake on the output of the Basal Ganglia [BG] in a diffuse manner to globally suppress the striatal system's ability to gate any motor behavior. Disruptions of normal STN activities by ablation, Deep Brain Stimulation and optogenetics result in failure to inhibit prepotent responses which lead to impulsive and potentially incorrect responses [54, 44, 45, 55, 56, 58, 59, 52, 57]. These results are consistent with network level models of BG function [38, 60, 14]; see also [87] which predicted that increases in STN firing dynamically raise the decision threshold to arrest premature responding, conceptually buying the executive system time to resolve the conflict and implement the appropriate action.

Despite the growing body of work on STN dynamics, the electrophysiological mechanisms of these dynamics remain poorly understood. Many studies have shown that in conditions of response conflict, frontal and STN theta power is elevated [27, 88, 28, 29, 48], with frontal theta granger causal of STN theta [89]. Variability in such signals is related to transient global suppression of motor activity [46] and an increase in the effective decision threshold, manifest by slower but more accurate choices [27, 48, 29, 89, 90, 47]. But how are such theta-band signals generated in STN and under which conditions do they arise? An answer to such questions is critical not only in their own right but for advancing our understanding of the functional role of this system. For example, while the above studies showed positive relationships between STN theta and RT slowing during high conflict conditions, these correlations are in the opposite direction during low conflict conditions [27, 48], thus questioning theta power *per se* as indexing the need for response caution.

Extending prior models [73, 74], we have developed a novel biophysically principled [91] large scale model of the subthalamopallidal circuit, including arkypallidal and prototypic units, with sparse and probabilistic connectivities [76, 36, 78, 92, 93, 94, 95, 83, 86], to query the conditions under which low frequency oscillations would emerge. Many factors, including conductance dynamics of individual cells [96, 97, 98, 36, 99, 81, 84] and network topography [68, 67, 69, 70, 71, 72], could potentially influence STN theta power. Moreover, even if theta signals are already observed in cortex, since neural communication is essentially nonlinear and discontinuous, it is non-trivial how observed frontal theta translates into cortical spiking to synaptically drive STN theta. Another compounding difficulty is the lack of understanding of cortical spiking under conflict condition. Given that the level of response conflict is a key determinant of when theta leads to increases in reaction times, we consider various regimes of cortical to STN input, including burst events and rhythmic activities [97] that could constitute conflict conditions, and vary the topographical connectivities from motor cortical units to STN to see how they impact theta.

Our simulations show that NMDA-dependent mechanisms, including glutamatergic evoked triphasic response characterized by spiking, pause and bursting [100, 101, 92], robustly give rise to theta in response to cortical conflict. Further, this process is enhanced in the presence of coincidence detectors created by topographically overlapping motor programs

with STN subpopulations.

## 2.2 Materials & Methods

### 2.2.1 Overview of STN-GPe Network

We constructed a large scale model of the STN-GPe network to understand the conditions under which the STN exhibits changes in theta and spiking. Since STN activity is predominantly patterned by the reciprocal excitatory and inhibitory interactions with the GPe [36, 98, 78], we focus on the subthalamopallidal network whilst leaving out many key contributors of Basal Ganglia physiology such as the striatum and the globus pallidus internus. Nevertheless, to compensate for these limitations, our model tuning was challenged by biophysical constraints at various levels; we assume that the baseline activities of the GPe subpopulations represent the net effects of the non-modeled nuclei. We have also prioritized the ionotrophic effects of the synaptic transmission while leaving out metabotropic ones, mainly because of lack of data to tune cellular dynamics.

Consistent with reported population ratios [76, 77], our model consisted of 300 STN and 900 GPe cells simulated as point neurons with Hodgkin-Huxley based active ionic conductances [73]. Our network size was constrained by the sparse connectivities [36, 78] 2.1A which requires a large enough network to have enough synaptic interactions, and the simulation step of 0.0025 ms (dictated by the GPe stiff dynamics) which restricted the size due to computational resources limitations.

The GPe network contained two different cell subtypes [83, 86]: 600 prototypic (GPeP) and 300 arkypallidal (GPeA). Cells were randomly connected with predefined probabilities as shown in Fig. 2.1A and described further below. The cells and synapses were tuned, via several iterations, to reproduce a baseline state that represents a healthy condition where the units in the network fire asynchronously within and across the populations (see Fig. 2.1 B, C, E) with symmetrically and normally distributed spiking rates with means for STN, GPeP and GPeA set around 11 [102, 103, 99], 30 and 5 spikes/s respectively [79, 80, 81, 82, 83, 84, 85, 86]. To further constrain our parameter sets, we analyzed the membrane potentials of the cells in the network and used only those that showed realistic

| Description | Parameter | Value | Unit |
|---|---|---|---|
| STN $Na^+$ conductance | $g_{Na}$ | 45 | $mS/cm^2$ |
| STN $K^+$ conductance | $g_K$ | 30 | $mS/cm^2$ |
| STN $Na^+$ $m-$gate half activation voltage | $\theta_m$ | -35 | $mV$ |
| GPeP $Na^+$ $h-$gate kinetics factor | $\phi_h$ | 0.04 | |
| GPeP $K^+$ $n-$gate kinetics factor | $\phi_n$ | 0.04 | |
| GPeP $Ca^{2+}$ pump rate | $k_{Ca}$ | 15.0 | |
| GPeA $Na^+$ conductance | $g_{Na}$ | 100 | $mS/cm^2$ |
| GPeA $K^+$ conductance | $g_K$ | 33 | $mS/cm^2$ |
| GPeA $Na^+$ $h-$gate kinetics factor | $\phi_h$ | 0.006 | |
| GPeA $K^+$ $n-$gate kinetics factor | $\phi_n$ | 0.006 | |
| GPeA $Ca^{2+}$ pump rate | $k_{Ca}$ | 15.0 | |

Table 2.1: **Parameters for cellular spontaneous activity.** Symbols are same as in Terman, Rubin, Yew, and Wilson [73]. Their GPe dynamics relates to the GPe Prototypic, GPeP, in this study. The dynamics of the novel GPe Arkypallidal, GPeA, cells have been adapted from the tuned GPeP.

non-pathological voltage traces.

To investigate the influence of cortical activity, the STN cells were driven with trains of spikes that activated excitatory AMPA and NMDA synapses, as described below.

Our simulations used the Neuron framework in Python with MPI parallelization [104, 91] and were run on the High Performance Computing resources at Brown University and XSEDE resources [105, 106, 107].

### 2.2.2 Individual Cell Models

STN and GPeP cells were modeled as in Terman, Rubin, Yew, and Wilson [73], with the $Na^+$, $K^+$, $leak$, $L-type\ Ca^{2+}$, $T-type\ Ca^{2+}$, and $[Ca^{2+}]-dependent\ K^+$ currents and active conductances. Note that the GPe described in Terman, Rubin, Yew, and Wilson [73] corresponds to our GPeP units, and we made parameter adjustments to the GPeP units to model the novel GPeA cells. This addition was motivated not only because GPeP and GPeA have very different firing rates but also due to the fact that GPeP send reciprocal inhibition to the STN, whereas the GPeA do not. All equations and parameters for STN and GPeP were as in Terman, Rubin, Yew, and Wilson [73] and Rubin and Terman [74], except for changes detailed in Tab. 2.1.

Since baseline firing rates depend on both cellular dynamics and synaptic conductances

(see section 2.2.3), we performed manual tuning to settle on the parameter set that met our biophysical constraints.

The original STN model [73] had autonomous firing rate around 2 spikes/s, and to have an in-network average firing rate of 11 spikes/s for the STN, we first tried to get the baseline state by changing the synaptic conductances after fixing their kinetics (see section 2.2.3), but parameter searches in the synaptic conductance space yielded no solution. We then proceeded by incorporating constant current clamps in the models. While these did increase the firing rates to the desired levels, the subsequent subthreshold activities and action potential shapes were significantly altered by these physiologically implausible depolarizing forces, which also reduced the ability of the synaptic inputs to influence postsynaptic behaviors. Increasing synaptic conductances to alleviate the latter effects, in fact, led to more pathological membrane potential trajectories, particularly in action potential generation and shape. To circumvent all these issues, we eventually modified the intrinsic dynamics of the cells as detailed in Tab. 2.1.

Based on membrane potential traces, we adjusted the STN's firing threshold to -8 mV from Neuron's default value of 0. The stiff dynamics of the GPe cells dictated our simulation timestep of 0.0025 ms. We downsampled our data to 0.025 ms for storage in 32-bit binary format in the HDF5 hierarchical structure [108]. All spiking and STN synaptic data were stored.

### 2.2.3 STN-GPe Synaptic Connections

Each STN unit had a GABA synapse for responding to GPeP stimulation. Both GPeP and GPeA cells had an AMPA and an NMDA presynaptically connected to the STN, and a GABA synapse that was triggered by GPeP and GPeA activities. The different units were probabilistically connected as shown in Fig. 2.1A with the values in square boxes indicating the sparse connection probabilities (Bernoulli trial), based on previous reports [92, 93, 94, 95, 36, 78, 85, 86].

In contrast to solving the first-order differential model in Terman, Rubin, Yew, and Wilson [73] and Rubin and Terman [74], we opted for the computationally less expensive biexponential model, Neuron's Exp2Syn mechanism [113], for synaptic responses, which has already

| Property | S-GX_A | S-GX_N | GP-X | GP-S | C-S_A | C-S_N |
|---|---|---|---|---|---|---|
| Synapse | AMPA | NMDA | GABA | GABA | AMPA | NMDA |
| $\bar{g_V}$ [pS] | 0.15 | 0.225 | 100 | 8 | var | var |
| $\tau_{rise}$ [ms] | 0.83 | 5.5 | 0.89 | 0.875 | 0.83 | 5.5 |
| $\tau_{decay}$ [ms] | 4.53 | 48 | 4.75 | 7.72 | 4.53 | 48 |
| $E_{syn}$ [mV] | 0 | 0 | -65 | -84 | 0 | 0 |
| $\delta_{syn}$ [ms] | 4.9 | 4.9 | 1 | 4.75 | 5 | 5 |
| $a$ | 1 | 0 | 0 | 0 | 1 | 0 |
| $b$ | -1 | 1 | 1 | 1 | -1 | 1 |
| $V_{1/2}$ [mV] | 30 | -36 | -39 | -9 | 30 | -36 |
| $k$ | 0.045 | 0.06613 | 0.5 | 0.125 | 0.045 | 0.06613 |
| *Ref.* | | | [109, 110] | [78, 111] | [101, 112] | [112] |

Table 2.2: **Parameters for synaptic models.** Key: S=STN, GP=GPeP, GX={GPeP, GPeA}, A=AMPA, N=NMDA. Code: S-GX_A refers to the AMPA (A) synapse on both GPeP and GPeA (GX) units with STN (S) as presynaptic unit. Note: Due to unavailability of data, we have assumed the kinetics and conductance voltage dependence for the glutamatergic synapses on GPe subpopulations to be the same as those on the STN.

an analytic solution. However, we modified the model to allow maximal conductances, $\bar{g_V}$, to be dependent on voltage for capturing I-V characteristics. To control the dynamic range, saturation and positive/negative relationship for the voltage dependent maximal conductance, we used a logistic model,

$$g_{syn}(V) = a + \frac{b}{1 + e^{-k(V - V_{1/2})}},$$

with parameters described in Tab. 2.2.

Despite its simplicity, the biexponential model does not have a closed-form solution to solve for the (10-90%) rise $\tau_{rise}$, and decay $\tau_{decay}$ rates. In order to replicate the time courses of synaptic responses under voltage clamps, we manually fit the biexponential model by guessing an initial solution of time rises and decays to achieve the 10-90% characteristics, iteratively refining the ranges to converge upon a satisfying solution, which are reported in Tab. 2.2

$E_{syn}$ was the reversal potential of each synaptic channel. Our synaptic activities used the Neuron's NetCon mechanism with transmission delays, $\delta_{syn}$. Due to unavailability of data, we have assumed the kinetics and conductance voltage dependence for the glutamatergic

synapses on GPe subpopulations to be the same as those on the STN since they are all subcortical structures.

Our baseline network tuning of cellular and synaptic activities minimized the incidence of synchronous STN and GPe firing (see Fig. 2.1B and C) in network since such synchrony is characteristic of pathological conditions [114, 115, 98, 36, 116].

### 2.2.4 Cortex to STN connectivity

#### Tuning Synapses

Each STN unit had an AMPA and an NMDA synapses for cortical responses. The cortico-STN synaptic parameters, Tab. 2.2, were tuned as above and matched the data from Chu, Atherton, Wokosin, Surmeier, and Bevan [112], both for kinetics and maximal conductance voltage dependence. The latter formalism also helped to capture the rectifying effects of $Mg^{2+}$ block in NMDA dynamics. The NMDA to AMPA maximal conductance ratio was kept at 1.402.

Due to unavailability of cortical spiking data in response conflict condition, we adopted two models of spiking profiles, Fig. 2.3(A,B,D,E) that have been described [97] to underlie frequency band power modulation: a rhythmic mode and a burst event mode. In rhythmic mode, the spikes were generated at fixed time periods, $T_{per}$, (driving frequency, $f_{drv} = 1/T_{per}$) while in Burst Event mode, the spikes were generated as Bursts with short Inter-Burst-Intervals (IBI) drawn from a Gaussian distribution, with the event lasting over some fixed duration, $E_{Dur}$.

We drove the network rhythmically with frequencies in the range from 2 through 32 Hz to cover both theta and non-theta drives. We simulated the Burst Event over a wide range of durations [10-250] ms and by varying the mean IBI and the standard deviation to the Gaussian, we could create Low [IBI: mean = 9 ms, std = 6 ms] and High [IBI: mean = 3 ms, std = 2 ms] Stim Burst conditions.

Based on initial observations that replicated physiologically plausible synaptic responses and non-pathological action potentials, we varied the NMDA conductances in the range from 1 through 40 nS, with the values 3.66, 18.3 and 36.6 referred to as Low, Mid and High

NMDA respectively.

### Cortico-STN architecture

We assumed that cortical drive to the STN, referred to as cortical "feed", either Rhythmic or Burst Event, coded for a particular motor program, and each feed innervated the STN units in the reported somatotopic organization [67]. We divided our STN population into four subpopulations, and probabilistically connected the cortical feeds to units in each subpopulation, as described below. Since subpopulations conceptually represented somatotopic areas, motor programs coding for mutually exclusive behaviors would thus preferentially innervate their own target subpopulations.

To investigate the effect of such preferential STN targeting on theta power, we parametrically varied the connection probability of a cortical feed to its own STN subpopulation. When the cortical feed connected exclusively to its own subpopulation, consequently segregating the cortico-STN communication, we call it a Segregated Topography, Fig. 2.7, with target probability, $p_{tar}$, 1 (the cortical feed drives all the STN units in the subpopulation) and non-target probability $p_{non-tar}$, 0. A Non-Segregated Topography was defined by allowing cortical feeds and STN subpopulations to crosstalk by varying the value of $p_{tar}$ in the set (0.85, 0.55 and 0.25) under the constraint $p_{tar} + 3 \times p_{non-tar} = 1$ to ensure that the total expected synaptic connections stayed the same across all levels of segregations. This disambiguated the contributions of cortico-STN topography from cortical input energy on STN theta power.

Note that $p_{tar} = 1$ represented a fully organized columnar topography while $p_{non-tar}$ a fully random one. The probabilistic connectivities in Non-Segregated cases gave rise to STN units that received from more than one cortical feed, and they were termed coincidence detectors, Fig. 2.7 C, since they could listen to multiple motor programs.

### Simulating Conflict

To simulate Conflict conditions, we presented the network with two different cortical Burst Events, each preferentially targeting a distinct STN subpopulation; contrast Fig. 2.7D, and E with H and H respectively.

To vary the levels of Conflict, we varied the durations $E_{dur}$ of the feeds, and the delay $\delta$ and overlap $\cap$ between cortical feeds, Fig. 2.7H. For a High Conflict condition, we used a duration of 50 ms and High Stim Bursts for both cortical feeds.

Since experiments reported that cortical theta could be Granger causal to STN theta [88, 29], we tested the effects of rhythmic cortical burst events by implementing the cortical stimulation profiles in Fig. 2.7I.

### 2.2.5 Analysis

Custom Python scripts were written for all analyses.

#### Spectral Analysis

Spectral analysis was performed on simulated local field potentials (LFP). As a proxy for LFP, we use the net synaptic currents across the population of interest. To contrast single STN unit LFP with no synaptic activity from GPeP, we used the net capacitative currents instead, only for the panels of Fig. 2.2. Specifically, LFP was calculated as the mean of the sums of synaptic currents across all cells in the population of interest at every recorded time point. Spectral analysis was performed using the complex Morlet wavelet method, which was generated using Scipy and further normalized to ensure that the net input energy of the Morlet wavelet across various frequencies was controlled for. For every frequency in the range of 2 through 64 Hz (logarithmically distributed), we calculated the complex Morlet signal with 3.5 cycles and $2^{17}$ (equivalent to around 3.3 s long kernel) points at a sampling period of 0.025 ms to create a time frequency spectrogram.

For efficiency, we opted for spectral domain multiplication using the Scipy fftconvolve routine after demeaning our time series data. The amplitudes of the resulting process were squared and treated as spectral power. To compute the power of a specific band, we average over all the frequencies that are members of that band at every time points.

Resonant frequency was defined as the frequency that showed highest power.

### Spike Statistics

All raster plots shown represented the recorded spike times directly. The latter were directly used to compute the Inter Spike Intervals, ISIs, for every unit in the network.

To compute population spike counts, we first discretized the spiking data of each cell in fixed bin sizes of 5 ms, and the aggregates in each bin were taken over all STN units that constituted a population of interest.

For cumulative spiking, we used the above spike counts for each subpopulation and cumulatively add them over succeeding time bins. To estimate the increase in spiking rate over the stimulation period, we divided the total number of spikes over that period by the total duration of the stimulation. For rhythmic bursts, the inter burst intervals were also counted as part of the stimulation duration.

Silence of STN units was defined as the first ISI that followed the first spiking evoked by cortical stimulation. We averaged over all STN units in a subpopulation as a measure of population silence.

Burst rates, were calculated by counting the number of spikes over a fixed time interval, usually 200 ms, immediately after the silence period, and averaged as above.

### Statistical Analysis

We performed simple two-tail Welch's T-test (SciPy Stats) between pairs of conditions, each with matched number of trials, for both average theta power and average spiking rates, and we used a significance level of 0.05.

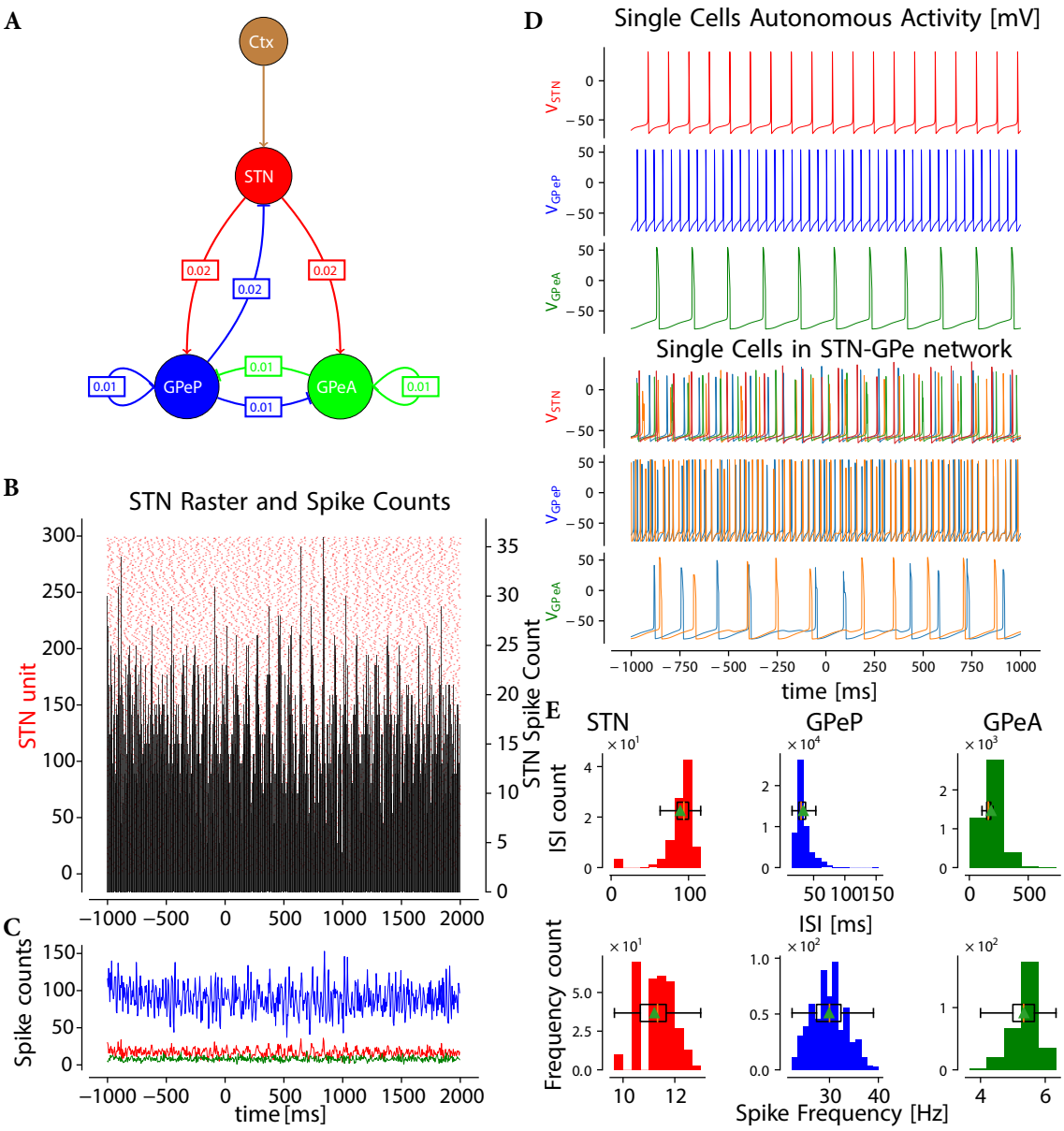


Figure 2.1: **Baseline state of subthalamopallidal network A** The subthalamopallidal network model consists of 300 STN (red), 600 prototypic (blue) and 300 arkypallidal (green) GPe single compartment units with Hodgkin-Huxley based dynamics, and probabilistically connected as shown. Numbers in the squares indicate the sparse connection probabilities between populations. **B** Raster plot of a typical network with no cortical input for all 300 STN units are shown in red. The spike counts (dark gray) are the sum of spikes in 5 ms time bins and show that the network fires asynchronously both within and across subpopulations. **C** The spike counts for all three subpopulations (color matched to A) show that only a proportion of the units happen to fire in the same 5 ms time bins. **D** Membrane potentials for each cell type after tuning. Top three rows represent the autonomous activities of each isolated cell (color as in A). Bottom three rows show typical examples of each cell embedded in the subthalamopallidal network (with no cortical input). **E** Top: Histograms of ISIs. Bottom: Histogram of firing rates.

## 2.3 Results

We first explore the biophysical properties, and impact of synaptic conductances and cortical inputs on LFPs and spikes. We then proceed to simulate architectural effects of cortico-STN topography on STN theta, and how they change under conflict condition.

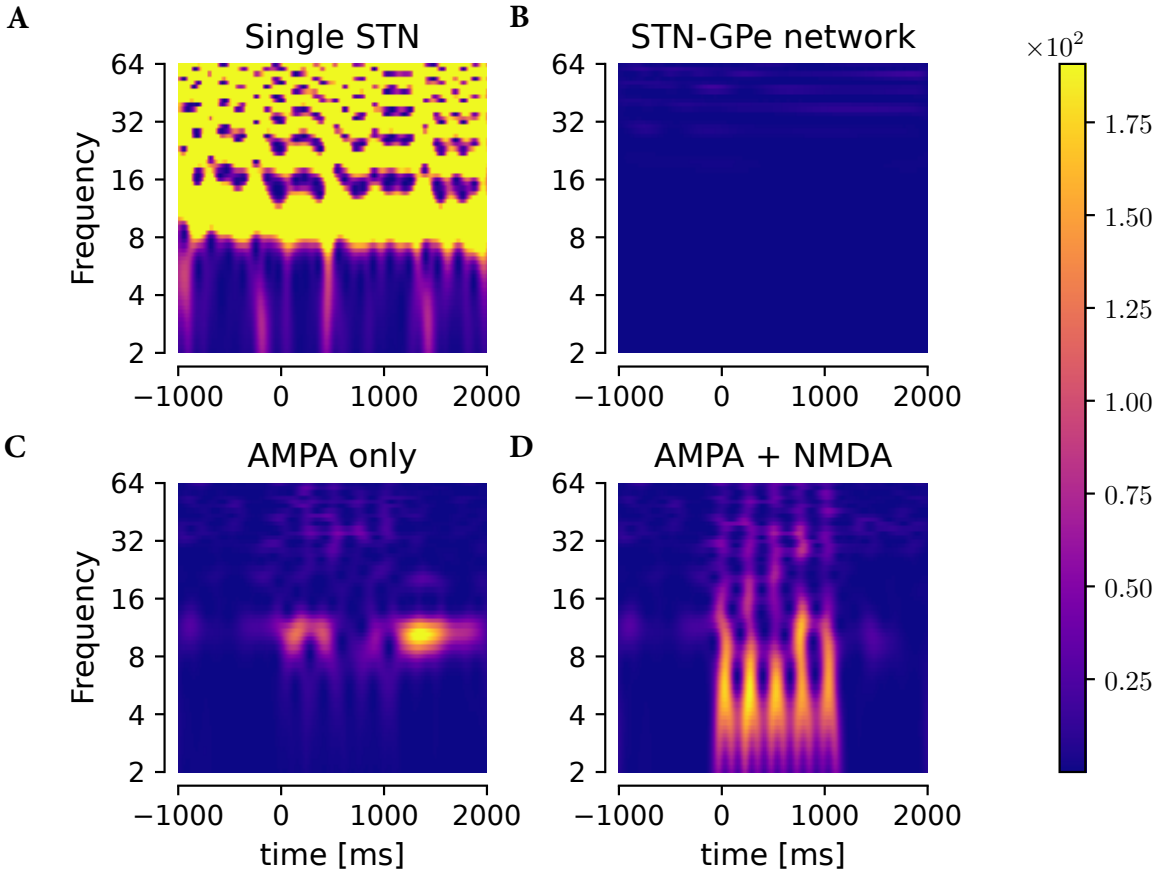


Figure 2.2: **NMDA currents give rise to STN theta power in response to cortical input** Each panel shows spectrograms for the net capacitative currents under different conditions. **A** Single STN unit with no synaptic input shows higher frequency signals but does not spontaneously show theta activities. **B** Aggregate STN LFP does not show theta activity in subthalamopallidal network without cortical drive. **C** 4Hz rhythmic cortical drive is provided to the STN. Under NMDA blockade, AMPA currents are not sufficient for theta band expression under cortical drive. Same results hold for cortical burst events (not shown). **D** NMDA currents are both necessary and sufficient for theta resonance; example same as in C. Other simulations show that NMDA alone (i.e., with AMPA blockade) is sufficient for STN to resonate in theta band (data not shown).

### 2.3.1 The Subthalamopallidal network requires cortically-driven NMDA currents to show theta band resonance.

We first checked whether our adapted STN model, tuned to replicate in-network average firing rate of 11 spikes/s, showed any theta band activity in its net capacitative currents in the isolated neuron (i.e., unconnected network), based on its autonomous pacemaking activity. In this setting, the STN unit showed only higher frequency band activities, Fig. 2.2A.

We next investigated whether subthreshold activities in the STN units would show theta power due to reciprocal GPe interactions within the tuned (Fig. 2.1 A,E) subthalamopallidal network. We averaged the net capacitative currents of all STN units and computed the spectrograms from spectral power similar to the spectral analysis of net synaptic currents described in the methods. Once again, no theta band power was observed, as shown in Fig. 2.2B. Since the network was probabilistically connected, we ran several (n=15) instantiations; the absence of theta band activity was consistent across all such trials (data not shown).

We then tested if and how cortical inputs to the network could drive theta band rhythmicity. Cortical drive was simulated either periodically over a fixed length of time or by providing a burst of activities over a short duration, Fig. 2.2. To elucidate the contributions of the cortically-driven glutamatergic synaptic currents, we ran the simulations with either AMPA or NMDA blockade. Simulations show that cortically-driven AMPA currents alone do not generate theta band resonance (see Fig. 2.2C for an example of 4 Hz rhythmic drive. However, theta resonance emerged with the addition of NMDA synapses, Fig. 2.2D (same 4 Hz drive), and persisted with the removal of AMPA currents (data not shown) and under burst event drive (described below). As such, NMDA activity was both necessary, Fig. 2.2D, and sufficient for theta band resonance.

### 2.3.2 Cortical bursts are filtered by NMDA dynamics to robustly elicit theta band activity

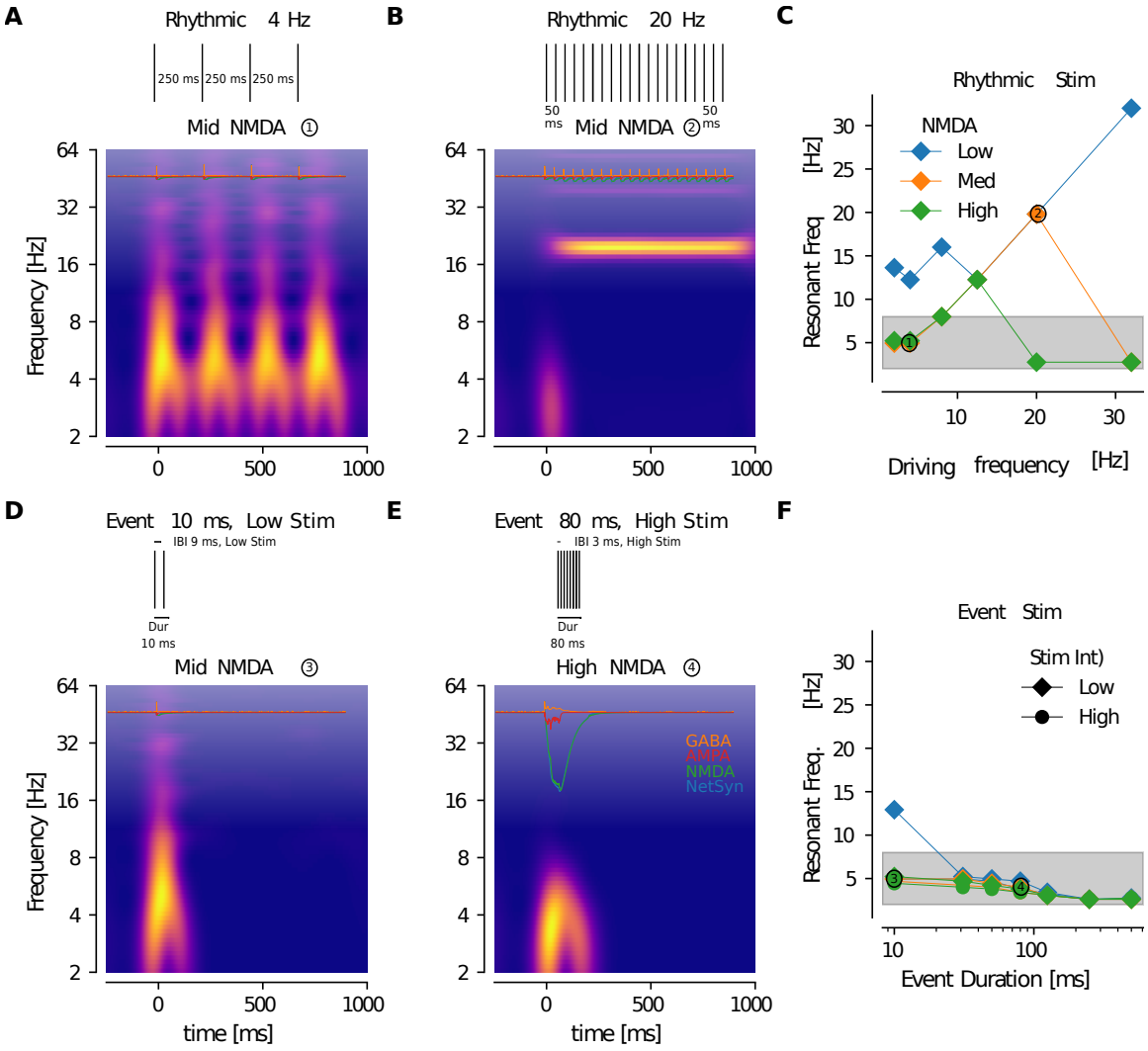


Figure 2.3: **Cortical dynamics alter STN theta expression** Panels **A-D** show spectrograms of net synaptic currents (small overlays, see panel E for legends) of STN units under different cortical dynamics. Results shown for mid NMDA level (see Methods). **A, B** When cortical inputs are rhythmic, the resonant STN frequency follows the driving frequency. **D, E** For cortical burst events, theta is robustly expressed over a wide range of cortical dynamics, such as event durations and burst intensities. **C, F** Nonlinear interactions of NMDA conductance on resonant frequency in rhythmic **C** and burst events **F**. Circled numbers on plots correspond to exemplar spectrograms A-D.

A standard way to investigate resonance in nonlinear systems with feedback connections is to analyze its response to rhythmic external drives. We drove the network across a range of frequencies (2, 4, 8, 12.5, 20 and 32 Hz), to examine which might produce theta band

activity. We observed that the STN showed resonance at the driving frequency, Fig. 2.3A, B. When the network was driven rhythmically at 4 Hz with mid-NMDA level, both synaptic activities showed theta band activity pattern (see Fig. 2.3A, insets). In this case, we also observed spiking rates (not shown here) following the 4 Hz pattern. The synaptic activities for a similar 20 Hz drive again showed resonance at the driving frequency, Fig. 2.3B, but the cortical activity did not entrain STN spiking at 20 Hz (not shown).

We then tested the effects of cortical burst event patterns, as might occur during brief periods of response conflict; [39, 40]. The duration and burst intensities of the events were varied to contrast a 'Low Stim' protocol (10 ms duration and inter burst interval of 9 ms, Fig. 2.3D) with a 'High Stim' protocol (80 ms duration, 3 ms inter burst interval, Fig. 2.3E). Despite this huge variability in burst events, both simulations yielded resonance in theta power. Interestingly, the resonant frequency in the High Stim case was lower than in the Low Stim case.

While both rhythmic and burst events were able to produce theta band activities, these findings were differentially dependent on NMDA conductances, Fig. 2.3C,F. In the rhythmic driving mode, high NMDA conductance was needed to support resonance in the lower driving frequencies, whereas low NMDA conductance favored resonance at the higher driving frequencies. In contrast, burst event stimulations yielded theta band resonance over all three levels of NMDA and a wide range of durations (albeit with lower resonant frequencies with longer event durations and higher burst spiking, as described above).

### 2.3.3 A cortically-evoked triphasic response in STN units is mediated by NMDA currents.

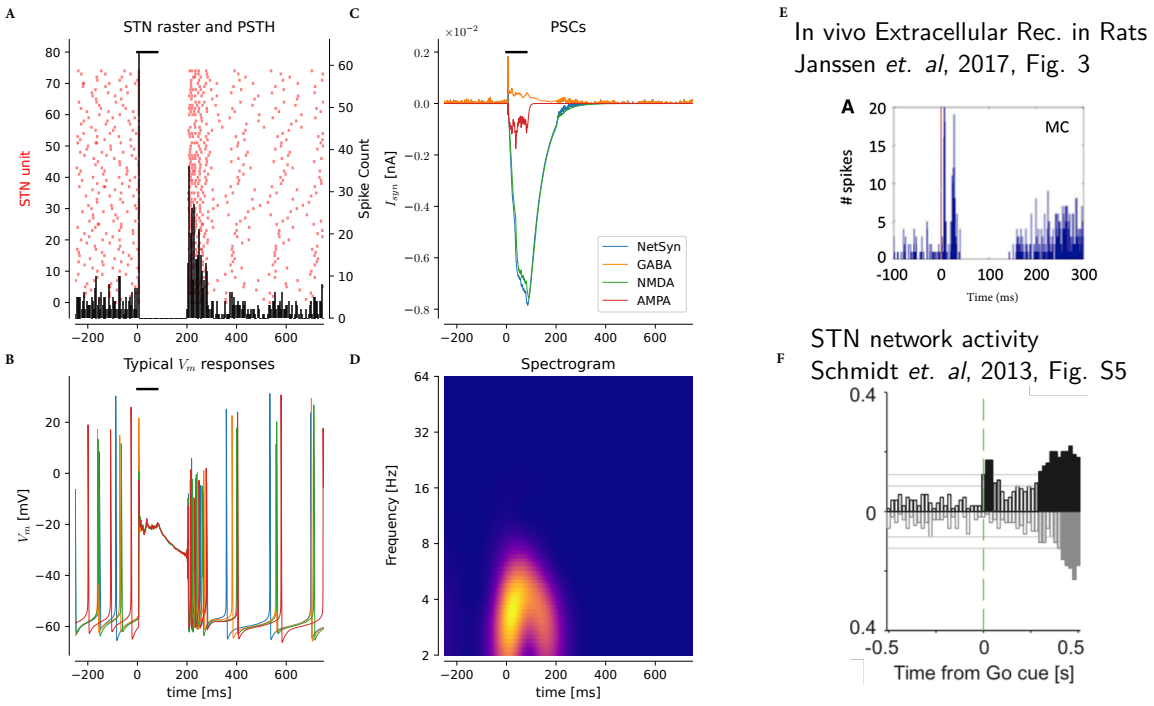


Figure 2.4: **STN shows triphasic response to cortical stimulation A** STN raster plot and spike counts demonstrate the triphasic response following cortical stimulation, characterized by initial spiking, pause in firing and finally, bursting behavior. Black bars represent duration of cortical burst event. **B** Typical STN voltage traces underlying triphasic response. After initial spiking, the cell exhibits depolarization block during which it remains near-20 mV, followed by a slow relaxation until spiking resumes in burst mode. **C** STN synaptic currents and **D** Spectrogram of net synaptic currents shows that the silence period within the triphasic response aligns with large amplitude NMDA currents and corresponding emergence of theta. **E, F** Experimental evidence of triphasic response in *in vivo* conditions at cellular **E** and network **F** levels.

Consistent with empirical reports in both primates and rodents [117, 100, 114, 118, 119, 42], following cortical stimulation, STN units in our model responded with a triphasic response characterized by spiking, followed by a pause and then finally bursts, Fig. 2.4A. Of note, we did not tune the parameters to exhibit this experimental observation, Fig. 2.4E,F; it emerged due to the biophysical constraints we incorporated in the design of the network (Methods).

Notably, while one might expect that the silent period was induced by inhibition, the pause

in firing occurred simultaneously with the time course of the NMDA currents. We analyzed individual STN membrane potential traces, Fig. 2.4B, and found that this phenomenon was due to a depolarization block mechanism that was induced by the rising amplitude of the NMDA current followed by a long recovery period , Fig. 2.4C, that temporally aligned with the decay period. Once the NMDA currents decayed enough for GPe-mediated GABAergic currents to be effective in influencing the cells, we observed subthreshold oscillations in the membrane potential followed by burst firing (which were also NMDA dependent, as described below). Finally, since the NMDA currents dominated the generation of the resonant theta frequency response, the duration of theta band resonance, Fig. 2.4D, corresponded with the pause duration.

We further investigated how the activities in each phase depended on the synaptic conductances (GABA and NMDA) in response to cortical spiking. We first confirmed that increases in GPe GABAergic conductance had no effect on the initial spiking but increased the pause durations [114] and reduced the burst activities (data not shown). For NMDA, larger conductances had no effect on initial spiking, and counterintuitively, larger NMDA conductances also prolonged the silence period. Phase space analysis revealed that this effect was due to the excitatory postsynaptic currents inducing a blockage of potassium currents, thus precluding hyperpolarization to enable action potential generation. Finally, the post-silence bursts showed a nonlinear concave relationship with NMDA. One possible explanation comes from contrasting the time courses of NMDA mediated depolarization block during silence and L-type gating dynamics. As NMDA conductance increases, it helps in accelerating depolarization and L-type current activations, which lead to bursts once the silence period terminates. However, under larger NMDA conductances, the pauses are so prolonged that by the time the cell is ready to fire, the L-type currents have deactivated, producing even fewer burst spikes.

### 2.3.4 STN burst firing depends on nonlinear interactions between NMDA and cortical spike timings

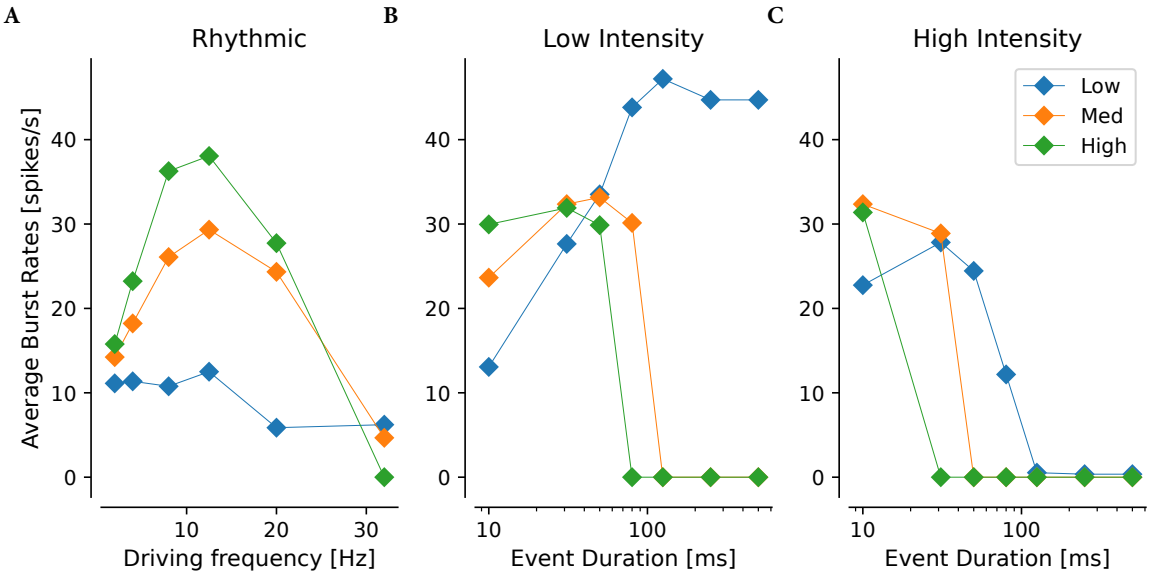


Figure 2.5: **Nonlinear effects of NMDA and cortical dynamics on STN bursting** **A** Under cortical rhythmic mode, STN burst rates showed an inverted-U relationship with driving frequency, which is consistent across all NMDA levels. **B** Under a low intensity cortical burst event, lower NMDA currents promote greater STN bursting and a wider dynamic range. **C** In contrast, high intensity cortical events show lower STN bursting and saturate faster with higher NMDA levels.

We also analyzed the STN burst rates, part of the third phase of the triphasic response, following the same types of cortical drive. In the rhythmic cortical mode, Fig. 2.5A, higher NMDA yielded more spiking at fixed driving frequencies, up to 20hz ($f \leq 20$). However, the relationship between bursting activities and driving frequencies showed an inverted-U shape for all NMDA levels, such the that highest spiking occurred near 12.5Hz.

In the bursting cortical model, high intensity bursts, Fig. 2.5C, led to saturation of STN spiking with longer event durations; the rate at which this occurred increased with NMDA levels. There was thus greater dynamic range in STN spiking with lower NMDA levels, Fig. 2.5B.

### 2.3.5 Theta power is strongly modulated by conflict and cortical to STN topography

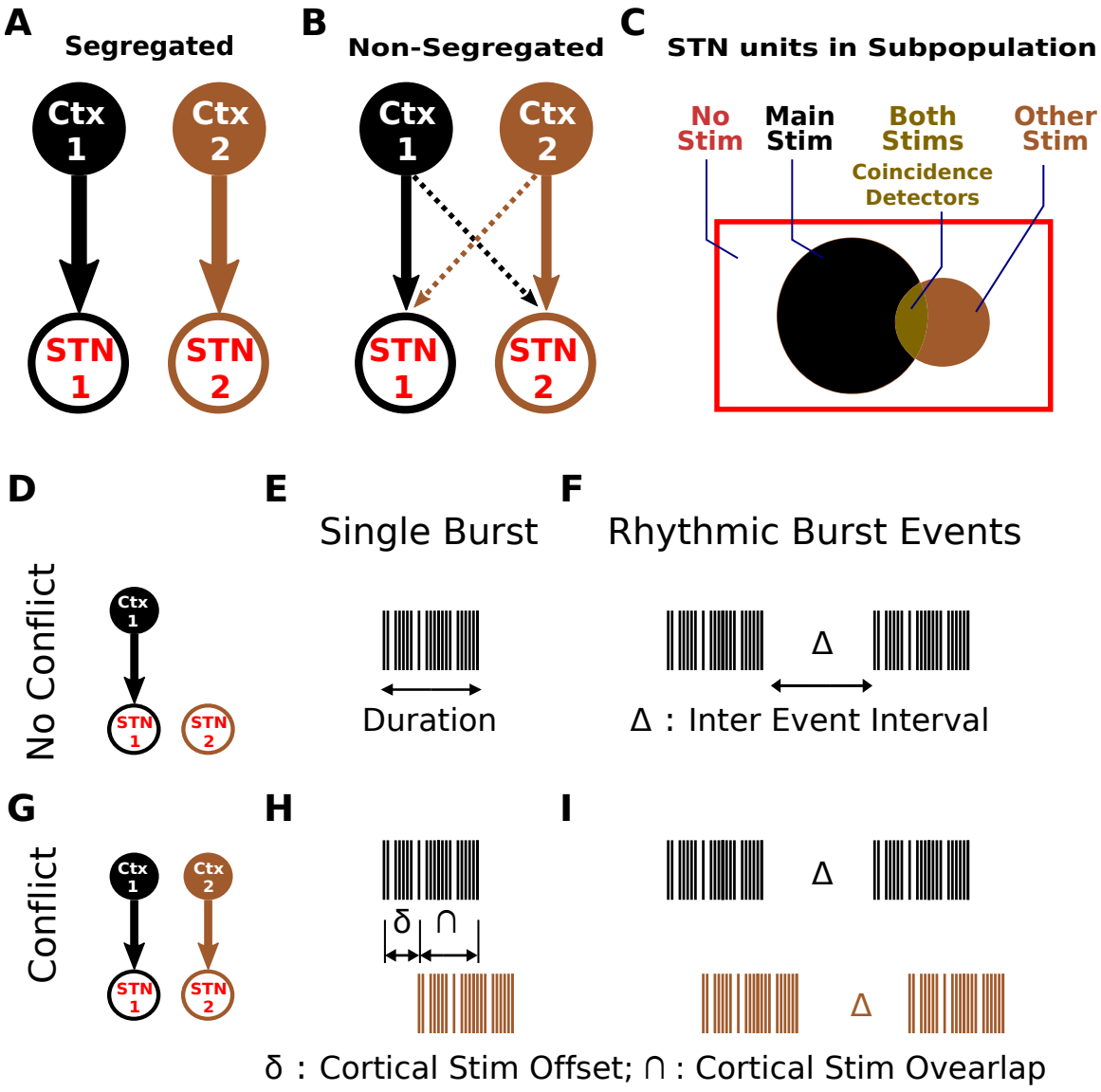

Figure 2.6: **Simulating variations in architecture (cortico-STN topography) and cortical dynamics of response conflict A-C** STN subpopulations receive input from cortical populations representing distinct motor actions, but the connectivity can be varied probabilistically from fully segregated to fully divergent. **A** In a fully segregated topography, a given cortical population projects to a single subpopulation only, implying that information is segregated through an organized columnar architecture. **B** In a non-segregated scheme, cortical information is probabilistically divergent across STN subpopulations. **C** The non-segregated network gives rise to four distinct classes of STN units depending on their cortical inputs. Due to probabilistic connectivity, the majority of units receive from a single cortical population, but others may receive from neither or both populations. The latter act as coincidence detectors. Lower levels of segregation lead to a greater proportion of coincidence detector units. The total connections were held constant across levels of segregation. **D, G** Varying levels of cortical response conflict. In the no conflict condition, a single cortical drive **D** is active and projects to its corresponding STN population. In the conflict condition, two cortical populations are co-activated **G**. **E, H** Each cortical event was simulated as a burst of spikes. In the conflict condition, these events overlapped in time. **F, I** These cortical events were also presented rhythmically to simulate vacillations in action selection over time (repeated bouts of conflict contrasted against repeated bouts of no conflict).

With a clearer understanding of how NMDA was involved in theta power modulation, we proceeded to test how cortico-STN topography and simulated response conflict impact theta power using various simulation protocols Fig. 2.6. To simulate response conflict, we considered conditions in which two populations of motor units (representing mutually incompatible responses) were coactive with varying temporal delays, compared to low or no conflict (only a single population active). We varied topography of cortical inputs from completely segregated (each cortical population projects to a single STN subpopulation) to fully random connections (each STN unit is equally likely to receive inputs from any motor population). Note that as the topography is more random and less segregated, the number of STN units that receive inputs from more than one population increases. We posited that the presence of such "coincidence detectors" would facilitate the encoding of response conflict in the STN and that this would impact low frequency oscillations in accordance with the literature (see introduction). Having established that cortical burst drive was more efficient at driving theta, here we consider only burst drive either as single events or repeated "rhythmic" burst events, Fig. 2.6E,F,H,I.

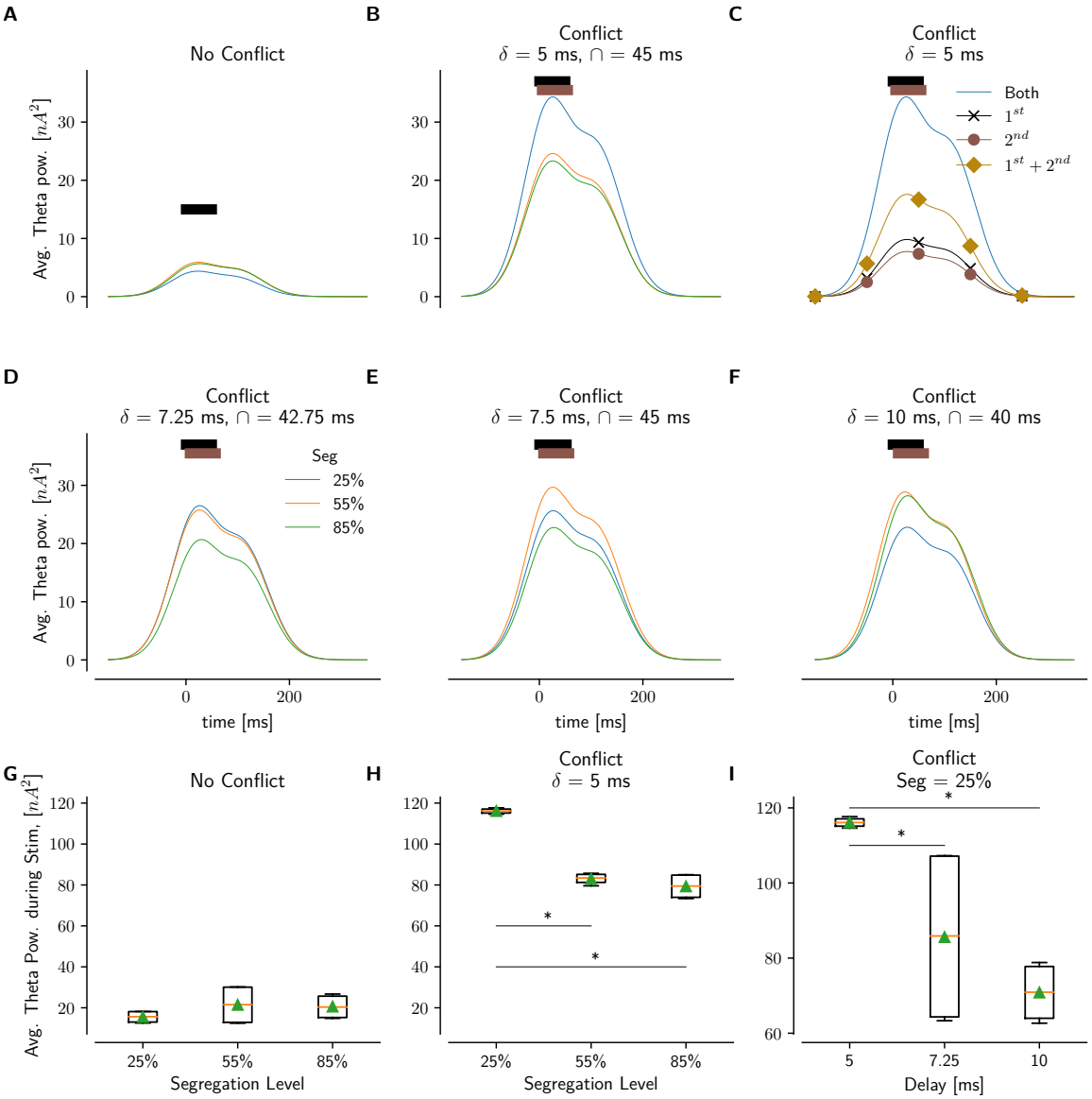


Figure 2.7: **Cortico-STN topography interacts with conflict to enhance STN theta power. A, G** Under no conflict condition, STN theta was limited and if anything, showed little variability with segregation. **B** STN theta was magnified with conflict and increasing numbers of coincidence detectors (lower segregation levels) **C** In coincidence detector units, theta power was larger than the sum of that across two populations that each received single cortical inputs. **D** The relationship between theta power and segregation levels was most prevalent when the delay between the two cortical feeds was low (0-7.25ms), thus highlighting the need for co-activation. **F**. Controlling for the temporal overlap of cortical drives **B, E**, at the delay of 10 ms, theta power was maximized not by the lowest segregation but by the intermediate level. **G-I** Box and whisker plots, green triangle: mean value, orange line: median value, significance level at 0.05. Average theta power during stimulation **G,H** In no conflict condition, there was no significant monotonic relationship between theta and segregation **G,A**, while theta showed significant negative correlation with segregation H,B under high conflict condition with very short delay (5ms). I Increasing the delay while keeping stimulation intensity and durations constant lead to lower theta power at the lowest segregation levels.

To understand the relationship between segregation levels and theta power, we considered a high conflict situation, whereby two cortical populations were simultaneously driven (offset by 0-15ms) with equally long and intense bursts). Notably, theta power increased with more coincidence detectors (lower segregation). Note that this result is not simply due to more input; indeed, we maintained the total number of inputs to the STN to be equal across all levels of segregation. An example of such high conflict with a delay between two cortical events ($\delta$) of 5ms is shown in Fig. 2.7B,H (two-sided Welch's T-test, $p<0.05$).

These results recapitulate the dominant finding in the human STN LFP literature, whereby response conflict increases STN theta power. To test whether the presence of coincidence detectors mediate the increased theta, we computed the average theta power in STN subpopulations, Fig. 2.6. We found that indeed, theta power was elevated in coincidence detectors at all segregation levels. This finding stems from a supralinear summation afforded by the biophysical properties of the STN network: theta power in coincidence detectors was greater than the sum of power in two populations that each received from only one cortical feed (see Fig. 2.6C for an example).

To further investigate whether the above effects are specific to response conflict *per se* we manipulated the temporal overlap between the populations, given a definition of conflict in terms of the co-activation of mutually incompatible responses, or Hopfield energy [12, 13, 38]. We manipulated the delays between cortical inputs for $\delta = 0$, 2.5, 5, 7.25, 10, 12.5, 15, 75 and 125 ms. We found that theta power was maximized in the unsegregated network (more coincidence detectors) for the lowest delays: from 0 through 7.25 ms, Fig. 2.6B,D,I (two-sided Welch's T-test, $p<0.05$ for short delay of 5 ms). Beyond this delay, there was an inverted-U effect, in which theta was largest for mid levels of segregation, Fig. 2.6F. Controlling for the overlap at 45 ms, Fig. 2.6 B,E, the mid level of segregation gave the maximum theta. For long enough delays with no overlap (no conflict), the highest level of segregation yielded the most theta power (not shown).

Finally, we considered a condition without any conflict at all: a single high stimulation burst event of 50 ms duration was fed to the network. These results converge with those above with long delays, whereby theta power was maximal with higher levels of segregation, Fig. 2.7A,G (two-sided Welch's T-test, no sig. diff.), and was somewhat reduced in the presence

of "coincidence detector" units (given that there was no coincidence to detect during no conflict).

These results are notable in that the literature implicates higher theta powers that are linked to higher RT levels during response conflict, but that this pattern is not seen – and indeed is often reversed – in low conflict situations [48, 27]. An interpretation from the model is that higher theta power during low conflict situations reflects greater activity in segregated subpopulations that simply recapitulate cortical inputs from a single dominant response, in which case the STN is not needed to pause behavior. Indeed, DBS and STN manipulations have little to no effect on responses in low conflict situations (see discussion).

### 2.3.6 Rhythmic Burst Events at theta frequency maximize STN spiking and theta power

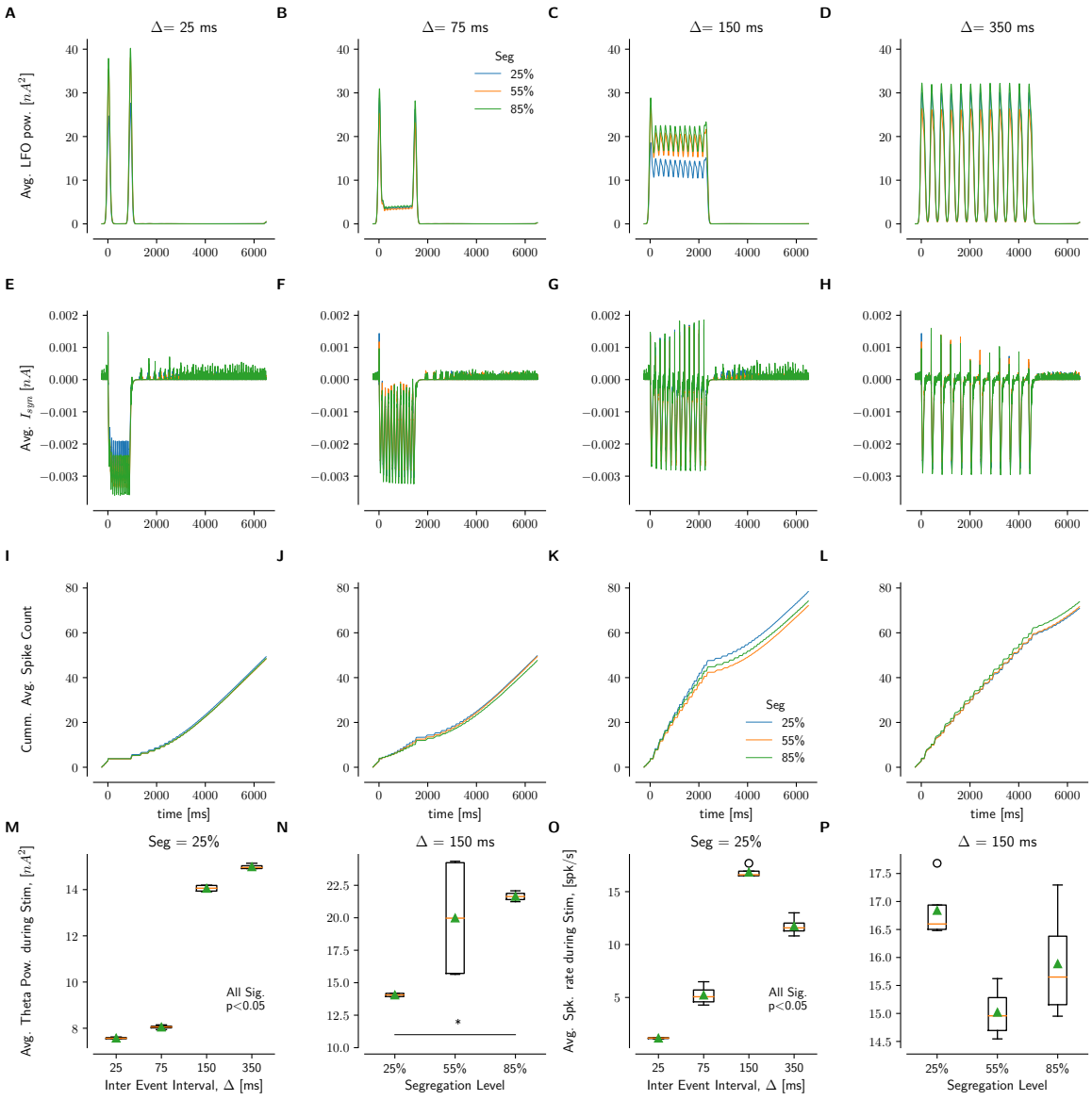

Figure 2.8: **Rhythmic bursts of cortical conflict induce prolonged STN theta and increased spiking. A-D** Rhythmic burst events (see Fig. 2.6F, I) lead to longer theta power. **C** Prolonged theta was observed when the inter event interval (IEI) between bouts of conflict was 150 s (i.e., in the theta range). Other IEIs produce only transient peaks in theta. **A**. Increasing the IEI to 75 ms **B** helped sustain theta at low amplitudes while a large IEI of 350 ms **D** allowed larger rhythmic amplitudes but less sustained theta. **E-H** Corresponding synaptic currents at various segregation levels. **E, G** The synaptic currents reached larger peaks for IEI = 25 ms but the theta range (IEI of 150 ms) allowed for sufficient time for NMDA currents to relax such that subsequent events could generate higher current amplitudes in an oscillatory manner, contributing to higher theta power in spite of lower peak values. **F** An IEI of 75 ms showed intermediate amplitude, while increasing IEI to 350 ms **H** allowed higher oscillatory current amplitudes. **I-L** Cumulative spiking of STN coincidence detector units. Rhythmic burst events with IEI in theta range, 150 ms, **K**, provided higher firing rates as compared to 25, 75 and 350 ms IEIs **I,J,L**. **M-P** Box and whisker plots, green triangle: mean value, orange line: median value, significance level at 0.05. **M,N** Average theta power during stimulation. **O,P** Average spiking rates during stimulation **M,O** Effect of inter event interval at fixed segregation level = 25% (more coincidence detectors). **N,P** Effect of segregation level at fixed IEI in theta range, 150 ms.

In the above simulations, we observed that STN theta power could be expressed either by rhythmic cortical inputs in the theta range or by burst events, especially with conflict. However, we also noted that higher theta power was associated with lower STN spiking (longer pauses in the triphasic response). This latter result is counterintuitive because several studies have shown increased STN spike rates during conflict which correlate with larger decision thresholds [48, 40, 41]. To investigate a possible reconciliation of these observations, we first noted that STN bursting occurred only after NMDA currents decayed, which also signaled the end of theta band resonance. We then assessed the impact of prolonged response conflict in which rhythmic and burst event modes are combined, representing a situation in which conflict persists for multiple cycles in cortex, Fig. 2.6I. We used the same high stimulation burst event (50 ms duration, 3 ms inter burst interval, 12 burst events), and then tested the impact of having these conflicting events repeat at different inter-event intervals, with $\Delta$, tested at 25, 75, 150 and 350 ms. Notably, 150ms falls in the theta range period.

We first tested the rhythmic event spiking (12 burst events per cortical feed) in the no conflict condition as above, and observed that, unlike in the previous case, theta power did not differ significantly across segregation levels (results not shown). When $\Delta$ was 150 ms

(theta range), theta power peaked due to being sustained for a longer period, and, critically, this also increased STN firing. While interburst intervals of 75 and 200 ms resulted in spike rates similar to the 150 ms condition, their theta powers were significantly lower.

Next, we presented two simultaneous rhythmic event drives (12 burst events per drive) to examine the influence of conflict in the network, Fig. 2.6. Theta power was higher for every inter burst interval as compared to the no conflict condition, as expected. While the peak amplitudes of instantaneous theta power decreased with IEI, Fig. 2.6A, B, C, they became more sustained at increasingly higher amplitudes, leading to overall net theta power, Fig. 2.6N. With an IEI of 200 ms, we saw larger amplitudes with no sustained activity. Nevertheless, theta power increased because the rhythmicity of the instantaneous theta activity lied in the theta band, Fig. 2.6D. We then predicted that larger IEI would elicit rhythmic activities outside of theta band. Indeed, for IEI of 450 ms, we found that overall theta power was lower (not shown) due to less sustained activity, despite achieving peak oscillatory instantaneous power.

To understand the mechanisms underlying the different instantaneous theta power dynamics, we analyzed the net synaptic currents from which theta power were calculated. For the large and brief theta powers, e.g. IEI 25 ms, the currents were high in magnitudes but lower in oscillatory amplitudes, thus explaining why the brief bursts of theta power occurred at the start and end of cortical stimulations, Fig. 2.6E, F. Instantaneous theta was sustained because the synaptic currents themselves oscillated in theta band, Fig. 2.6H, consequently contributing additional theta power. In the case of IEI of 350 ms, the currents had enough time to decay to basal levels before being synaptically driven. Since these could be viewed as successions of single events, each burst event contributed to theta resonance by virtue of NMDA dynamics, Figs. 2.3D-F, 2.4C, D. We observed significant effects of segregation on theta power between the lowest and highest tested conditions only, Fig. 2.6N.

Since STN spiking increases during response inhibition [40], we tested the effects of IEI on spiking. We found that average spike rates peaked for IEI of 150 ms (theta range) Fig. 2.6O, and these were significant across all segregation levels (shown here for the lowest 25%, maximum conflict detectors). For any fixed IEI, we did not observe significant effects of segregation, Fig. 2.6P, but the firing rates at the lowest segregation tended to be higher,

suggesting that having more coincidence detectors is important for spiking and thus braking behaviors. In fact, the high spiking rates were maintained across IEI of 125 through 200 ms, corresponding to the higher end of the theta frequencies.

These results are consistent with observations that cortical theta is Granger causal of STN theta, while also accounting for STN-GPe cellular and network dynamics that mediate changes in spiking.

## 2.4 Discussion

Our simulation studies provide a novel theoretical framework for interpreting the mechanistic basis behind the growing body of evidence linking low frequency oscillations in the STN to conflict and decision threshold adjustment [29, 28, 89, 120, 48, 90, 27, 121, 47, 59, 57, 46]. Such findings accord with existing neural network models of basal ganglia, in which STN spike rates are elevated during response conflict, which, by modulating BG output structures and thalamocortical activity, gives rise to a transient increase in decision threshold [38, 14, 60]; see also [87]. However, such models do not provide insight into the source and role of low frequency rhythms *per se*. The current biophysical explorations of STN-GPe circuitry advances our understanding of the underlying mechanisms, leading to the following novel and testable conclusions.

First, our model shows that power in low frequency (e.g., theta) band does not spontaneously emerge in the STN-GPe circuit, but rather require cortical input. Second, low frequency power is strongly dependent on NMDA currents; AMPA currents alone were insufficient. Third, we found that the dynamics of cortical input were important for determining net theta power: STN neurons could exhibit theta band resonance if the cortical inputs themselves oscillate in theta [28, 29, 88, 46], but they also emerged robustly in response to cortical burst events at a broad range of intensities and durations, particularly when such events overlapped (mimicking conflict). Moreover, both low frequency power and STN spiking were particularly elevated and prolonged when these two cortical modes were combined during rhythmic burst events, representing a state of conflict in which cortical motor plans oscillate back and forth in the theta range. These findings accord with the

literature, whereby individual STN neurons exhibit increased spike rates to conflicting evidence [40, 41]. Finally, theta band resonance was also strongly modulated by architectural constraints, with maximal response when cortical inputs provided divergent connectivity to multiple STN subpopulations. Analysis of the underlying mechanism of such effects revealed an NMDA-dependent supralinear response in STN "coincidence detector" units.

### 2.4.1 NMDA Mechanisms of Subthalamic Theta Band Power

The dependence on cortically-driven NMDA currents for theta band power expression is explained by the slow time courses of the NMDA currents, which were biophysically constrained from the literature. For rhythmic drives, the oscillatory nature of the NMDA-dominated synaptic currents dictated the resonant frequency. Conversely, in the case of single burst events, theta band resonance emerged due to the time period of the envelope of the decaying phase of the NMDA current. Both of these effects combined during rhythmic burst events, contributing to sustained theta power. Notably, while theta band resonance is often described in terms of low frequency "oscillations" , our investigations align with biophysical models demonstrating how resonance can also emerge from burst events and not just rhythmic activities, Jones [97].

On the applied end, such findings imply that it may be possible to enhance STN function in tasks that require cognitive control by targeting local NMDA receptors, particularly the NR2D subtype which is most prevalent in STN and GPe [122, 123]. Indeed, these authors have recently developed a Positive Allosteric Modulator that target NR2D and showed that in rats, it effectively reduced premature responding in a response conflict task. It is notable that such premature responding to conflict is common in rats with STN lesions [45, 44] and indeed, this phenomenon was a motivating influence on the theory that STN implements a "hold your horses" mechanism in systems level neural models [38]. Our biophysical model provides a rationale for why NMDA currents per se would influence such function, and moreover suggest that yet stronger doses could reverse the effect due to depolarization block and thus reduce the decision threshold rather than increasing it. Thus, in principle, different doses of such an agent could be useful for both disorders of impulsivity (too low decision threshold) and compulsivity (too high).

### 2.4.2 Cortico-STN communication and implication for encoding conflict

When connectivity from cortical to STN subpopulations was fully segregated (i.e., no coincidence detector units), we found that theta band resonance depended only on the overall intensity of cortically driven NMDA currents. However, with increased presence of coincidence detector units, while preserving the sum total of cortical inputs, we found that STN theta was elevated particularly when cortical inputs from multiple populations overlapped in time (i.e., conflict). The primate STN is topographically organized by functional domains, namely motor, associative and limbic with broadly defined boundaries though there also exist convergence zones that receive from more than one domain [69, 71, 72]. In addition, Nambu [67] describes two broadly separated somatotopic organizations within the motor domain, which receive mainly from M1 and SMA. Our findings regarding burst events suggest that STN units can respond to conflict among motor representations, based on the coactivation of cells that code for mutually exclusive behaviors, and hence some local cross-talk (i.e., imperfect segregation within the motor domain). However, STN also receives direct projections from dorsomedial frontal areas such as preSMA and anterior cingulate, regions that themselves detect conflict and resonate in theta [37, 29, 121]. Thus, our findings may have implications for both of these circuits, and suggest that STN theta band resonance would be maximal when they are combined (albeit here within the same cortical population).

### 2.4.3 Emergence of Triphasic response via NMDA depolarization block

Our biophysical model, while more detailed than extant models of STN-GPe (for example containing multiple GPe populations [85, 86]), is still simplified relative to the complexity of real STN units. Despite the simplicity of our synaptic models, our single compartment STN unit successfully reproduced the experimentally observed triphasic phenomenon in response to cortical stimulation, characterized by initial spiking, pause and subsequent bursting [100, 101, 92, 119, 124]. This dynamic behavior is believed to result from the STN spiking due to cortically-driven Glutamatergic excitatory postsynaptic currents, followed by inhibition from the GPe. The bursts are accounted for by rebound bursting due to T-type Calcium

currents activated by removal of GPe mediated hyperpolarization following cortico-striatal inhibition [114, 125, 92, 126]. Our investigations contribute an additional mechanistic explanation for such triphasic activity. Congruent with the extant interpretations, it is initiated by excitatory AMPA currents that promote initial spiking, and the onset of pause is triggered by synchronous recruitment of GABA activities from GPe. However, our model suggests that the pause is sustained beyond this inhibition due to the depolarization block induced by NMDA currents that weaken the effects of K+ currents, thereby preventing the hyperpolarization necessary for action potential generation. While this is prediction can be experimentally tested, it accords with previous studies [127, 128] that report depolarization block in the STN, and they stem from failure of potassium currents in regulating spiking behaviors. We observed that as long as cortical spiking persisted, the membrane potential was held at around -20 mV while NMDA current amplified. Once cortical spiking ceased, the NMDA current started to relax with a slow time course which prolonged the pause. Since the latter dynamics did not feature hyperpolarization, rebound bursting was due to depolarization activation of L-type Calcium currents. Although we do not focus on this in the present work, we have also varied GABA conductance from GPe and found that it prolongs the pause but, in contrast to the NMDA mechanism, reduces subsequent bursting.

### 2.4.4 Reconciling the theta-RT conundrum

While many studies have replicated the finding that low frequency oscillations are related to increases in response time and decision threshold, modulating the speed-accuracy tradeoff, it is noteworthy that all of these findings were specific to high conflict task conditions [29, 28, 89, 120, 48, 90, 27, 121, 47, 59, 46]. If frontal and STN theta band power is simply a "read out" of experienced conflict, then one should be able to predict RT from theta power irrespective of task condition. However, empirical findings have shown this to not be the case, but rather the opposite: within low conflict conditions, larger frontal and STN theta power is related to *reduced* RT [27, 48]. Nevertheless, evidence abound across species that STN is needed for stopping action rather than facilitating it [45, 37, 129, 40, 35, 52, 130, 46]. Our model provides two plausible mechanistic reconciliations of this observation.

First, we showed that during conflict conditions, increased theta was observed primar-

ily in coincidence detector units that signaled the co-activation of mutually incompatible responses. Indeed, theta power was stronger as a function of decreased segregation in cortico-STN connectivities. However, in low conflict situations, there was still an overall increase in theta with increased cortical intensity (driven by NMDA currents in individual STN populations), and this effect was actually stronger in networks with more segregation (less coincidence detectors). By this account, theta power during low conflict reflects strong cortical activation of a dominant response and hence preparation of a motor action. Increased theta at the population level does not necessarily involve increased spiking across the STN population. Indeed, empirical data show that STN spike rates increase in conflict conditions [40, 41], that STN theta suppresses motor activity and corticospinal excitability during conflict [46], and moreover, disrupting STN activity only impairs response inhibition during high conflict or surprising situations [55, 27, 57, 52]. Thus, we speculate that STN theta power during low conflict situations primarily reflects cortical input and is not suppressive on behavior either because overall net spiking is not increased, or because STN output is not effective at changing behavior during low conflict conditions. This last account is concordant with various evidence that basal ganglia is needed for modulation of action selection with internal volition but not when the correct action is sufficiently salient [8, 131, 31].

At the more biophysical level, note that our metric for theta was temporal summation of the spectral power, implying both magnitudes and durations matter. We found that in high conflict situations (low delays and high overlap between cortical feeds), nonlinear interactions between cortical spiking and NMDA caused the current to compound instead of summate temporally. This nonlinear summation amplifies NMDA current eliciting a rapid buildup of theta power. In contrast, during low conflict situations (longer delays between cortical feeds), the rate of buildup of the NMDA currents is slower, and can hence produce a negative theta-RT relationship.

### 2.4.5 Limitations and Future Directions

In these studies, we have provided both biophysical and architectural mechanisms associated with theta band power modulation by focusing on cortically evoked STN-GPe interactions.

We have deliberately not included other parts of the BG network including the striatum, in order to focus on the mechanisms of cortically driven theta power in STN which appear to be critical for modulating response time during conflict tasks. This does not imply that other parts of the network are irrelevant, and indeed it would be interesting to investigate the role of the D1 and D2 striatal pathways on GPe and STN communication, particularly as they are strongly implicated in motivated behavior.

# Bibliography


[1] H. Steiner and K. Tseng, *Handbook of Basal Ganglia Structure and Function*, ser. Handbook of Behavioral Neuroscience. Elsevier Science, 2010, ISBN: 9780080912158.

[2] S. R. Sesack and A. A. Grace, "Cortico-Basal Ganglia Reward Network: Microcircuitry," *Neuropsychopharmacology*, vol. 35, pp. 27–47, 2010.

[3] A. V. Kravitz, B. S. Freeze, P. R. L. Parker, K. Kay, M. T. Thwin, K. Deisseroth, and A. C. Kreitzer, "Regulation of parkinsonian motor behaviours by optogenetic control of basal ganglia circuitry," *Nature*, vol. 466, pp. 622–626, 2010.

[4] A. V. Kravitz, L. D. Tye, and A. C. Kreitzer, "Distinct roles for direct and indirect pathway striatal neurons in reinforcement," *Nat. Neurosci.*, vol. 15, pp. 816–818, 2012.

[5] T. Hikida, K. Kimura, N. Wada, K. Funabiki, and S. Nakanishi, "Distinct Roles of Synaptic Transmission in Direct and Indirect Striatal Pathways to Reward and Aversive Behavior," *Neuron*, vol. 66, pp. 896–907, 2010.

[6] E. A. Yttri and J. T. Dudman, "Opponent and bidirectional control of movement velocity in the basal ganglia," *Nature*, vol. 533, pp. 402–406, 2016.

[7] C. R. Gerfen and C. J. Wilson, "Chapter {II} The basal ganglia," in *Integr. Syst. CNS, part III Cerebellum, basal ganglia, olfactory Syst.* Ser. Handbook of Chemical Neuroanatomy, A. B. L.W. Swanson and T. HÖkfelt, Eds., vol. 12, Elsevier, 1996, pp. 371–468.

[8] P. Brown and C. Marsden, "What do the basal ganglia do?" *Lancet*, vol. 351, pp. 1801–1804, 1998.

[9] A. Reiner, L. Medina, and C. Veenman, "Structural and functional evolution of the basal ganglia in vertebrates," *Brain Res. Rev.*, vol. 28, no. 3, pp. 235–285, 1998.

[10] J. W. Mink, "The basal ganglia: focused selection and inhibition of competing motor programs," *Prog. Neurobiol.*, vol. 50, no. 4, pp. 381–425, 1996.

[11] P. Redgrave, T. J. Prescott, and K. Gurney, "The basal ganglia: a vertebrate solution to the selection problem?" *Neuroscience*, vol. 89, no. 4, pp. 1009–1023, 1999.

[12] M. M. Botvinick, T. S. Braver, D. M. Barch, C. S. Carter, and J. D. Cohen, "Conflict monitoring and cognitive control.," *Psychol. Rev.*, vol. 108, pp. 624–652, 2001.

[13] N. Yeung, M. M. Botvinick, and J. D. Cohen, "The Neural Basis of Error Detection: Conflict Monitoring and the Error-Related Negativity.," *Psychol. Rev.*, vol. 111, pp. 931–959, 2004.

[14] T. V. Wiecki and M. J. Frank, "A computational model of inhibitory control in frontal cortex and basal ganglia.," *Psychol. Rev.*, vol. 120, pp. 329–355, 2013.

[15] S. D. Berry and R. F. Thompson, "Prediction of learning rate from the hippocampal electroencephalogram," *Science*, vol. 200, no. 4347, pp. 1298–1300, 1978.

[16] U. Rutishauser, I. B. Ross, A. N. Mamelak, and E. M. Schuman, "Human memory strength is predicted by theta-frequency phase-locking of single neurons," *Nature*, vol. 464, no. 7290, pp. 903–907, 2010.

[17] A. Adhikari, M. A. Topiwala, and J. A. Gordon, "Synchronized Activity between the Ventral Hippocampus and the Medial Prefrontal Cortex during Anxiety," *Neuron*, vol. 65, pp. 257–269, 2010.

[18] S. Liebe, G. M. Hoerzer, N. K. Logothetis, and G. Rainer, "Theta coupling between V4 and prefrontal cortex predicts visual short-term memory performance," *Nat. Neurosci.*, vol. 15, no. 3, pp. 456–462, 2012.

[19] J. Larson, D. Wong, and G. Lynch, "Patterned stimulation at the theta frequency is optimal for the induction of hippocampal long-term potentiation," *Brain Res.*, vol. 368, no. 2, pp. 347–350, 1986.

[20] J. M. Hyman, B. P. Wyble, V. Goyal, C. A. Rossi, and M. E. Hasselmo, "Stimulation in hippocampal region CA1 in behaving rats yields long-term potentiation when delivered to the peak of theta and long-term depression when delivered to the trough," *J. Neurosci.*, vol. 23, no. 37, pp. 11 725–11 731, 2003.

[21] A. Terrazas, M. Krause, P. Lipa, K. M. Gothard, C. A. Barnes, and B. L. McNaughton, "Self-motion and the hippocampal spatial metric," *J. Neurosci.*, vol. 25, no. 35, pp. 8085–8096, 2005.

[22] J. Sarnthein, A. Morel, A. Von Stein, and D. Jeanmonod, "Thalamic theta field potentials and EEG: high thalamocortical coherence in patients with neurogenic pain, epilepsy and movement disorders," *Thalamus Relat. Syst.*, vol. 2, no. 03, pp. 231–238, 2003.

[23] Y.-Z. Huang, M. J. Edwards, E. Rounis, K. P. Bhatia, and J. C. Rothwell, "Theta burst stimulation of the human motor cortex," *Neuron*, vol. 45, no. 2, pp. 201–206, 2005.

[24] E. Başar, C. Başar-Eroglu, S. Karakaş, and M. Schürmann, "Gamma, alpha, delta, and theta oscillations govern cognitive processes," *Int. J. Psychophysiol.*, vol. 39, pp. 241–248, 2001.

[25] R. A. Moore, A. Gale, P. H. Morris, and D. Forrester, "Theta phase locking across the neocortex reflects cortico-hippocampal recursive communication during goal conflict resolution," *Int. J. Psychophysiol.*, vol. 60, no. 3, pp. 260–273, 2006.

[26] G. Tzur and A. Berger, "When things look wrong: Theta activity in rule violation," *Neuropsychologia*, vol. 45, no. 13, pp. 3122–3126, 2007.

[27] J. F. Cavanagh, T. V. Wiecki, M. X. Cohen, C. M. Figueroa, J. Samanta, S. J. Sherman, and M. J. Frank, "Subthalamic nucleus stimulation reverses mediofrontal influence over decision threshold," *Nat. Neurosci.*, vol. 14, pp. 1462–1467, 2011.

[28] B. Zavala, J.-S. J.-S. Brittain, N. Jenkinson, K. Ashkan, T. Foltynie, P. Limousin, L. Zrinzo, A. L. Green, T. Aziz, K. Zaghloul, and P. Brown, "Subthalamic Nucleus Local Field Potential Activity during the Eriksen Flanker Task Reveals a Novel Role

for Theta Phase during Conflict Monitoring," *J. Neurosci.*, vol. 33, no. 37, pp. 14 758–14 766, 2013.

[29] B. A. Zavala, H. Tan, S. Little, K. Ashkan, M. Hariz, T. Foltynie, L. Zrinzo, K. A. Zaghloul, and P. Brown, "Midline Frontal Cortex Low-Frequency Activity Drives Subthalamic Nucleus Oscillations during Conflict," *J. Neurosci.*, vol. 34, pp. 7322–7333, 2014.

[30] M. J. Frank, "Dynamic Dopamine Modulation in the Basal Ganglia: A Neurocomputational Account of Cognitive Deficits in Medicated and Nonmedicated Parkinsonism," vol. 17, no. 1, pp. 51–72,

[31] J. Cockburn, A. G. Collins, and M. J. Frank, "A Reinforcement Learning Mechanism Responsible for the Valuation of Free Choice," *Neuron*, vol. 83, pp. 551–557, 2014.

[32] M. D. Humphries, R. D. Stewart, and K. N. Gurney, "A physiologically plausible model of action selection and oscillatory activity in the basal ganglia," *J. Neurosci.*, vol. 26, no. 50, pp. 12 921–12 942, 2006.

[33] A. Nambu, H. Tokuno, and M. Takada, "Functional significance of the cortico–subthalamo–pallidal 'hyperdirect' pathway," *Neurosci. Res.*, vol. 43, no. 2, pp. 111–117, 2002.

[34] C. Bosch, P. Mailly, B. Degos, J.-M. Deniau, and L. Venance, "Preservation of the hyperdirect pathway of basal ganglia in a rodent brain slice," *Neuroscience*, vol. 215, pp. 31–41, 2012.

[35] S. Jahfari, F. Verbruggen, M. J. Frank, L. J. Waldorp, L. Colzato, K. R. Ridderinkhof, and B. U. Forstmann, "How Preparation Changes the Need for Top-Down Control of the Basal Ganglia When Inhibiting Premature Actions," *J. Neurosci.*, vol. 32, pp. 10 870–10 878, 2012.

[36] C. J. Wilson, "Subthalamo Pallidal circuit," in *Handb. brain microcircuits*, G. Shepherd and S. Grillner, Eds., Oxford: Oxford University Press, 2010.

[37] A. R. Aron, T. E. Behrens, S. Smith, M. J. Frank, and R. A. Poldrack, "Triangulating a cognitive control network using diffusion-weighted magnetic resonance imaging (MRI) and functional MRI," *J. Neurosci.*, vol. 27, no. 14, pp. 3743–3752, 2007.

[38] M. J. Frank, "Hold your horses: A dynamic computational role for the subthalamic nucleus in decision making," *Neural Networks*, vol. 19, pp. 1120–1136, 2006.

[39] M. Isoda and O. Hikosaka, "Switching from automatic to controlled action by monkey medial frontal cortex," *Nat. Neurosci.*, vol. 10, pp. 240–248, 2007.

[40] ——, "Role for Subthalamic Nucleus Neurons in Switching from Automatic to Controlled Eye Movement," *J. Neurosci.*, vol. 28, pp. 7209–7218, 2008.

[41] K. A. Zaghloul, C. T. Weidemann, B. C. Lega, J. L. Jaggi, G. H. Baltuch, and M. J. Kahana, "Neuronal Activity in the Human Subthalamic Nucleus Encodes Decision Conflict during Action Selection," *J. Neurosci.*, vol. 32, pp. 2453–2460, 2012.

[42] R. Schmidt, D. K. Leventhal, N. Mallet, F. Chen, and J. D. Berke, "Canceling actions involves a race between basal ganglia pathways," *Nat. Neurosci.*, vol. 16, pp. 1118–1124, 2013.

[43] S. Jahfari, L. Waldorp, W. P. M. van den Wildenberg, H. S. Scholte, K. R. Ridderinkhof, and B. U. Forstmann, "Effective Connectivity Reveals Important Roles for Both the Hyperdirect (Fronto-Subthalamic) and the Indirect (Fronto-Striatal-Pallidal) Fronto-Basal Ganglia Pathways during Response Inhibition," *J. Neurosci.*, vol. 31, no. 18, pp. 6891–6899, 2011.

[44] C. Baunez and T. W. Robbins, "Bilateral Lesions of the Subthalamic Nucleus Induce Multiple Deficits in an Attentional Task in Rats," *Eur. J. Neurosci.*, vol. 9, no. 10, pp. 2086–2099, 1997.

[45] C. Baunez, T. Humby, D. M. Eagle, L. J. Ryan, S. B. Dunnett, and T. W. Robbins, "Effects of STN lesions on simple vs choice reaction time tasks in the rat: preserved motor readiness, but impaired response selection," *European Journal of Neuroscience*, vol. 13, pp. 1609–1616, 2001.

[46] J. R. Wessel, D. A. Waller, and J. D. Greenlee, "Non-selective inhibition of inappropriate motor-tendencies during response-conflict by a fronto-subthalamic mechanism," *Elife*, vol. 8, 2019.

[47] R. Kelley, O. Flouty, E. B. Emmons, Y. Kim, J. Kingyon, J. R. Wessel, H. Oya, J. D. Greenlee, and N. S. Narayanan, "A human prefrontal-subthalamic circuit for cognitive control," *Brain*, vol. 141, pp. 205–216, 2018.

[48] D. M. M. Herz, B. A. A. Zavala, R. Bogacz, and P. Brown, "Neural Correlates of Decision Thresholds in the Human Subthalamic Nucleus," *Curr. Biol.*, vol. 26, pp. 916–920, 2016.

[49] W. Schultz, "Predictive Reward Signal of Dopamine Neurons," *J. Neurophysiol.*, vol. 80, no. 1, pp. 1–27, 1998.

[50] F. Verbruggen and G. D. Logan, "Automatic and controlled response inhibition: Associative learning in the go/no-go and stop-signal paradigms.," *J. Exp. Psychol. Gen.*, vol. 137, no. 4, pp. 649–672, 2008.

[51] K. R. Ridderinkhof, "The Role of the Medial Frontal Cortex in Cognitive Control," *Science*, vol. 306, no. 5695, pp. 443–447, 2004.

[52] K. H. Fife, N. A. Gutierrez-Reed, V. Zell, J. Bailly, C. M. Lewis, A. R. Aron, and T. S. Hnasko, "Causal role for the subthalamic nucleus in interrupting behavior," *Elife*, vol. 6, 2017.

[53] A. R. Aron, T. W. Robbins, and R. A. Poldrack, "Inhibition and the right inferior frontal cortex," *Trends Cogn. Sci.*, vol. 8, no. 4, pp. 170–177, 2004.

[54] C. Baunez, A. Nieoullon, and M. Amalric, "In a rat model of parkinsonism, lesions of the subthalamic nucleus reverse increases of reaction time but induce a dramatic premature responding deficit.," *J. Neurosci.*, vol. 15, no. 10, pp. 6531–41, 1995.

[55] M. J. Frank, J. Samanta, A. A. Moustafa, and S. J. Sherman, "Hold Your Horses: Impulsivity, Deep Brain Stimulation, and Medication in Parkinsonism," *Science*, vol. 318, pp. 1309–1312, 2007.

[56] S. A. Wylie, K. R. Ridderinkhof, W. J. Elias, R. C. Frysinger, T. R. Bashore, K. E. Downs, N. C. van Wouwe, and W. P. M. van den Wildenberg, "Subthalamic nucleus stimulation influences expression and suppression of impulsive behaviour in Parkinson's disease," *Brain*, vol. 133, no. 12, pp. 3611–3624, 2010.

[57] A. Ghahremani, A. R. Aron, K. Udupa, U. Saha, D. Reddy, W. D. Hutchison, S. K. Kalia, M. Hodaie, A. M. Lozano, and R. Chen, "Event-related deep brain stimulation of the subthalamic nucleus affects conflict processing," *Ann. Neurol.*, vol. 84, pp. 515–526, 2018.

[58] E. J. Coulthard, R. Bogacz, S. Javed, L. K. Mooney, G. Murphy, S. Keeley, and A. L. Whone, "Distinct roles of dopamine and subthalamic nucleus in learning and probabilistic decision making," *Brain*, vol. 135, no. 12, pp. 3721–3734, 2012.

[59] N. Green, R. Bogacz, J. Huebl, A.-K. Beyer, A. A. Kühn, and H. R. Heekeren, "Reduction of Influence of Task Difficulty on Perceptual Decision Making by STN Deep Brain Stimulation," *Curr. Biol.*, vol. 23, pp. 1681–1684, 2013.

[60] R. Ratcliff and M. J. Frank, "Reinforcement-Based Decision Making in Corticostriatal Circuits: Mutual Constraints by Neurocomputational and Diffusion Models," *Neural Comput.*, vol. 24, pp. 1186–1229, 2012.

[61] C. S. Carter, T. S. Braver, D. M. Barch, M. M. Botvinick, D. Noll, and J. D. Cohen, "Anterior Cingulate Cortex, Error Detection, and the Online Monitoring of Performance," *Science*, vol. 280, no. 5364, pp. 747–749, 1998.

[62] M. Botvinick, L. E. Nystrom, K. Fissell, C. S. Carter, and J. D. Cohen, "Conflict monitoring versus selection-for-action in anterior cingulate cortex," *Nature*, vol. 402, no. 6758, pp. 179–181, 1999.

[63] J. G. Kerns, J. D. Cohen, A. W. MacDonald, R. Y. Cho, V. A. Stenger, and C. S. Carter, "Anterior Cingulate Conflict Monitoring and Adjustments in Control," *Science*, vol. 303, no. 5660, pp. 1023–1026, 2004.

[64] A. W. MacDonald, J. D. Cohen, V. A. Stenger, and C. S. Carter, "Dissociating the Role of the Dorsolateral Prefrontal and Anterior Cingulate Cortex in Cognitive Control," *Science*, vol. 288, no. 5472, pp. 1835–1838, 2000.

[65] R. Giuffrida, G. L. Volsi, G. Maugeri, and V. Perciavalle, "Influences of pyramidal tract on the subthalamic nucleus in the cat," *Neurosci. Lett.*, vol. 54, no. 2–3, pp. 231–235, 1985.

[66] T. Kita and H. Kita, "The subthalamic nucleus is one of multiple innervation sites for long-range corticofugal axons: a single-axon tracing study in the rat," *J. Neurosci.*, vol. 32, no. 17, pp. 5990–5999, 2012.

[67] A. Nambu, "Somatotopic Organization of the Primate Basal Ganglia," *Front. Neuroanat.*, vol. 5, 2011.

[68] A. Mathai and Y. Smith, "The Corticostriatal and Corticosubthalamic Pathways: Two Entries, One Target. So What?" *Front. Syst. Neurosci.*, vol. 5, no. 64, 2011.

[69] W. I. A. Haynes and S. N. Haber, "The organization of prefrontal-subthalamic inputs in primates provides an anatomical substrate for both functional specificity and integration: implications for Basal Ganglia models and deep brain stimulation," *J. Neurosci.*, vol. 33, no. 11, pp. 4804–4814, 2013.

[70] H. Schroll and F. H. Hamker, "Computational models of basal-ganglia pathway functions: Focus on functional neuroanatomy," *Front. Syst. Neurosci.*, vol. 7, no. 122, 2013.

[71] T. Kita, P. Osten, and H. Kita, "Rat subthalamic nucleus and zona incerta share extensively overlapped representations of cortical functional territories," *J. Comp. Neurol.*, vol. 522, pp. 4043–4056, 2014.

[72] A. Alkemade, A. Schnitzler, and B. U. Forstmann, "Topographic organization of the human and non-human primate subthalamic nucleus," *Brain Struct. Funct.*, vol. 220, pp. 3075–3086, 2015.

[73] D. Terman, J. E. Rubin, A. C. Yew, and C. J. Wilson, "Activity patterns in a model for the subthalamopallidal network of the basal ganglia.," *J. Neurosci.*, vol. 22, pp. 2963–76, 2002.

[74] J. E. Rubin and D. Terman, "High Frequency Stimulation of the Subthalamic Nucleus Eliminates Pathological Thalamic Rhythmicity in a Computational Model," *J. Comput. Neurosci.*, vol. 16, pp. 211–235, 2004.

[75] R. Q. So, A. R. Kent, and W. M. Grill, "Relative contributions of local cell and passing fiber activation and silencing to changes in thalamic fidelity during deep brain stimulation and lesioning: a computational modeling study," *J. Comput. Neurosci.*, vol. 32, no. 3, pp. 499–519, 2012.

[76] D. E. Oorschot, "Total number of neurons in the neostriatal, pallidal, subthalamic, and substantia nigral nuclei of the rat basal ganglia: A stereological study using the cavalieri and optical disector methods," *J. Comp. Neurol.*, vol. 366, no. 4, pp. 580–599, 1996.

[77] C. D. Hardman, J. M. Henderson, D. I. Finkelstein, M. K. Horne, G. Paxinos, and G. M. Halliday, "Comparison of the basal ganglia in rats, marmosets, macaques, baboons, and humans: Volume and neuronal number for the output, internal relay, and striatal modulating nuclei," *J. Comp. Neurol.*, vol. 445, no. 3, pp. 238–255, 2002.

[78] J. Baufreton, E. Kirkham, J. F. Atherton, A. Menard, P. J. Magill, J. P. Bolam, and M. D. Bevan, "Sparse but Selective and Potent Synaptic Transmission From the Globus Pallidus to the Subthalamic Nucleus," *J. Neurophysiol.*, vol. 102, pp. 532–545, 2009.

[79] H. Kita and S. T. Kitai, "Intracellular study of rat globus pallidus neurons: membrane properties and responses to neostriatal, subthalamic and nigral stimulation," *Brain Res.*, vol. 564, no. 2, pp. 296–305, 1991.

[80] A. Nambu and R. Llinas, "Electrophysiology of globus pallidus neurons in vitro," *J. Neurophysiol.*, vol. 72, pp. 1127–1139, 1994.

[81] A. J. Cooper and I. M. Stanford, "Electrophysiological and morphological characteristics of three subtypes of rat globus pallidus neurone in vitro," *J. Physiol.*, vol. 527, no. 2, pp. 291–304, 2000.

[82] L. Benhamou, M. Bronfeld, I. Bar-Gad, and D. Cohen, "Globus Pallidus External Segment Neuron Classification in Freely Moving Rats: A Comparison to Primates," *PLoS One*, vol. 7, e45421, 2012.

[83] N. Mallet, B. R. Micklem, P. Henny, M. T. Brown, C. Williams, J. P. Bolam, K. C. Nakamura, and P. J. Magill, "Dichotomous Organization of the External Globus Pallidus," *Neuron*, vol. 74, pp. 1075–1086, 2012.

[84] C. A. Deister, R. Dodla, D. Barraza, H. Kita, and C. J. Wilson, "Firing rate and pattern heterogeneity in the globus pallidus arise from a single neuronal population," *J. Neurophysiol.*, vol. 109, pp. 497–506, 2013.

[85] K. J. Mastro, R. S. Bouchard, H. A. K. Holt, and A. H. Gittis, "Transgenic Mouse Lines Subdivide External Segment of the Globus Pallidus (GPe) Neurons and Reveal Distinct GPe Output Pathways," *J. Neurosci.*, vol. 34, pp. 2087–2099, 2014.

[86] A. Abdi, N. Mallet, F. Y. Mohamed, A. Sharott, P. D. Dodson, K. C. Nakamura, S. Suri, S. V. Avery, J. T. Larvin, F. N. Garas, S. N. Garas, F. Vinciati, S. Morin, E. Bezard, J. Baufreton, and P. J. Magill, "Prototypic and Arkypallidal Neurons in the Dopamine-Intact External Globus Pallidus," *J. Neurosci.*, vol. 35, pp. 6667–6688, 2015.

[87] R. Bogacz and K. Gurney, "The basal ganglia and cortex implement optimal decision making between alternative actions.," *Neural Comput.*, vol. 19, pp. 442–477, 2007.

[88] J. F. Cavanagh, J. L. Sanguinetti, J. J. B. Allen, S. J. Sherman, and M. J. Frank, "The subthalamic nucleus contributes to post-error slowing.," *J. Cogn. Neurosci.*, vol. 26, pp. 2637–2644, 2014.

[89] B. Zavala, H. Tan, S. Little, K. Ashkan, A. L. Green, T. Aziz, T. Foltynie, L. Zrinzo, K. Zaghloul, and P. Brown, "Decisions Made with Less Evidence Involve Higher

Levels of Corticosubthalamic Nucleus Theta Band Synchrony," *J. Cogn. Neurosci.*, vol. 28, pp. 811–825, 2016.

[90] D. M. Herz, H. Tan, J.-S. Brittain, P. Fischer, B. Cheeran, A. L. Green, J. FitzGerald, T. Z. Aziz, K. Ashkan, S. Little, T. Foltynie, P. Limousin, L. Zrinzo, R. Bogacz, and P. Brown, "Distinct mechanisms mediate speed-accuracy adjustments in cortico-subthalamic networks," *Elife*, vol. 6, 2017.

[91] S. R. Jones, "Biophysically Principled Computational Neural Network Modeling of Magneto-/Electro-Encephalography Measured Human Brain Oscillations," in *Neuronal Netw. Anal.* Ser. Neuromethods. 2012, vol. 67, pp. 459–485.

[92] M. D. Bevan, N. E. Hallworth, and J. Baufreton, "GABAergic control of the subthalamic nucleus," in *Prog. Brain Res.* Vol. 160, 2007, pp. 173–188.

[93] H. Kita, "Globus pallidus external segment," in *Gaba Basal Ganglia From Mol. to Syst.* Ser. Progress in Brain Research, E. D. A. James M. Tepper and J. P. Bolam, Eds., vol. 160, Elsevier, 2007, pp. 111–133.

[94] A. R. Sadek, P. J. Magill, and J. P. Bolam, "A Single-Cell Analysis of Intrinsic Connectivity in the Rat Globus Pallidus," *J. Neurosci.*, vol. 27, no. 24, pp. 6352–6362, 2007.

[95] H. Kita, "Organization of the Globus Pallidus," in *Handb. Basal Ganglia Struct. Funct.* G. Shepherd and S. Grillner, Eds., Oxford: Elsevier Inc., 2010.

[96] J. E. Rubin, "Computational models of basal ganglia dysfunction: the dynamics is in the details," *Curr. Opin. Neurobiol.*, vol. 46, pp. 127–135, 2017.

[97] S. R. Jones, "When brain rhythms aren't 'rhythmic': implication for their mechanisms and meaning," *Curr. Opin. Neurobiol.*, vol. 40, pp. 72–80, 2016.

[98] C. Wilson, "Active decorrelation in the basal ganglia," *Neuroscience*, vol. 250, pp. 467–482, 2013.

[99] M. D. Bevan and C. J. Wilson, "Mechanisms underlying spontaneous oscillation and rhythmic firing in rat subthalamic neurons.," *J. Neurosci.*, vol. 19, no. 17, pp. 7617–28, 1999.

[100] S. Kitai and J. Deniau, "Cortical inputs to the subthalamus: intracellular analysis," *Brain Res.*, vol. 214, pp. 411–415, 1981.

[101] P. J. Magill, A. Sharott, M. D. Bevan, P. Brown, and J. P. Bolam, "Synchronous Unit Activity and Local Field Potentials Evoked in the Subthalamic Nucleus by Cortical Stimulation," *J. Neurophysiol.*, vol. 92, no. 2, pp. 700–714, 2004.

[102] D. S. Kreiss, C. W. Mastropietro, S. S. Rawji, and J. R. Walters, "The response of subthalamic nucleus neurons to dopamine receptor stimulation in a rodent model of Parkinson's disease.," *J. Neurosci.*, vol. 17, pp. 6807–19, 1997.

[103] C. Beurrier, P. Congar, B. Bioulac, and C. Hammond, "Subthalamic Nucleus Neurons Switch from Single-Spike Activity to Burst-Firing Mode," *J. Neurosci.*, vol. 19, no. 2, pp. 599–609, 1999.

[104] M. L. Hines, A. P. Davison, and E. Muller, "NEURON and Python," *Front. Neuroinform.*, vol. 3, 2009.

[105] J. Towns, T. Cockerill, M. Dahan, I. Foster, K. Gaither, A. Grimshaw, V. Hazlewood, S. Lathrop, D. Lifka, G. D. Peterson, R. Roskies, J. R. Scott, and N. Wilkins-Diehr, "Xsede: Accelerating scientific discovery," *Computing in Science & Engineering*, vol. 16, pp. 62–74, 2014.

[106] S. Sivagnanam, A. Majumdar, K. Yoshimoto, V. Astakhov, A. Bandrowski, M. E. Martone, and N. T. Carnevale, "Introducing the neuroscience gateway.," in *IWSG*, 2013.

[107] T. Carnevale, A. Majumdar, S. Sivagnanam, K. Yoshimoto, V. Astakhov, A. Bandrowski, and M. Martone, "The neuroscience gateway portal: high performance computing made easy," *BMC Neurosci.*, vol. 15, P101, 2014.

[108] M. Folk, G. Heber, Q. Koziol, E. Pourmal, and D. Robinson, "An overview of the hdf5 technology suite and its applications," in *Proceedings of the EDBT/ICDT 2011 Workshop on Array Databases*, ACM, 2011, pp. 36–47.

[109] C. Miguelez, S. Morin, A. Martinez, M. Goillandeau, E. Bezard, B. Bioulac, and J. Baufreton, "Altered pallido-pallidal synaptic transmission leads to aberrant firing of globus pallidus neurons in a rat model of Parkinson's disease," *J. Physiol.*, vol. 590, pp. 5861–5875, 2012.

[110] J. Bugaysen, I. Bar-Gad, and A. Korngreen, "Continuous Modulation of Action Potential Firing by a Unitary GABAergic Connection in the Globus Pallidus In Vitro," *J. Neurosci.*, vol. 33, pp. 12 805–12 809, 2013.

[111] K. Y. Fan, J. Baufreton, D. J. Surmeier, C. S. Chan, and M. D. Bevan, "Proliferation of External Globus Pallidus-Subthalamic Nucleus Synapses following Degeneration of Midbrain Dopamine Neurons," *J. Neurosci.*, vol. 32, pp. 13 718–13 728, 2012.

[112] H.-Y. Chu, J. F. Atherton, D. Wokosin, D. J. Surmeier, and M. D. Bevan, "Heterosynaptic Regulation of External Globus Pallidus Inputs to the Subthalamic Nucleus by the Motor Cortex," *Neuron*, vol. 85, pp. 364–376, 2015.

[113] N. T. Carnevale and M. L. Hines, *The NEURON book*. Cambridge University Press, 2006.

[114] C. Hamani, "The subthalamic nucleus in the context of movement disorders," *Brain*, vol. 127, pp. 4–20, 2004.

[115] A. Eusebio, A. Pogosyan, S. Wang, B. Averbeck, L. D. Gaynor, S. Cantiniaux, T. Witjas, P. Limousin, J.-P. Azulay, and P. Brown, "Resonance in subthalamo-cortical circuits in Parkinson's disease," *Brain*, vol. 132, pp. 2139–2150, 2009.

[116] B. C. Schwab, T. Heida, Y. Zhao, E. Marani, S. A. van Gils, and R. J. A. van Wezel, "Synchrony in Parkinson's disease: importance of intrinsic properties of the external globus pallidus.," *Front. Syst. Neurosci.*, vol. 7, p. 60, 2013.

[117] M. L. F. Janssen, Y. Temel, C. Delaville, D. G. M. Zwartjes, T. Heida, P. De Deurwaerdère, V. Visser-Vandewalle, and A. Benazzouz, "Cortico-subthalamic inputs from the motor, limbic, and associative areas in normal and dopamine-depleted rats are not fully segregated," *Brain Struct. Funct.*, vol. 222, pp. 2473–2485, 2017.

[118] A. Nambu, H. Tokuno, I. Hamada, H. Kita, M. Imanishi, T. Akazawa, Y. Ikeuchi, and N. Hasegawa, "Excitatory Cortical Inputs to Pallidal Neurons Via the Subthalamic Nucleus in the Monkey," *J. Neurophysiol.*, vol. 84, pp. 289–300, 2000.

[119] A. Pautrat, M. Rolland, M. Barthelemy, C. Baunez, V. Sinniger, B. Piallat, M. Savasta, P. G. Overton, O. David, and V. Coizet, "Revealing a novel nociceptive network that links the subthalamic nucleus to pain processing," *Elife*, vol. 7, 2018.

[120] B. A. Zavala, A. I. Jang, and K. A. Zaghloul, "Human subthalamic nucleus activity during non-motor decision making," *Elife*, vol. 6, 2017.

[121] M. J. Frank, C. Gagne, E. Nyhus, S. Masters, T. V. Wiecki, J. F. Cavanagh, and D. Badre, "fMRI and EEG predictors of dynamic decision parameters during human reinforcement learning.," *J. Neurosci.*, vol. 35, pp. 485–94, 2015.

[122] F. Yi, Y. Xu, C. M. Fanger, E. Gordon, K. Paschetto, K. B. Hansen, F. S. Menniti, and R. A. Volkmann, "PTC-137, a positive allosteric modulator of NMDA receptors containing GluN2C or GluN2D subunits," in preparation.

[123] P. M. Callahan, J. A. V. Terry, F. R. Nelson, R. A. Volkmann, A. B. Vinod, M. Zannudin, and F. S. Menniti, "Modulating inhibitory response control through potentiation of GluN2D subunit-containing NMDA receptors," in preparation.

[124] N. Maurice, J.-M. Deniau, J. Glowinski, and A.-M. Thierry, "Relationships between the prefrontal cortex and the basal ganglia in the rat: physiology of the corticosubthalamic circuits," *J. Neurosci.*, vol. 18, no. 22, pp. 9539–9546, 1998.

[125] P. J. Magill, A. Sharott, J. P. Bolam, and P. Brown, "Delayed synchronization of activity in cortex and subthalamic nucleus following cortical stimulation in the rat," *J. Physiol.*, vol. 574, pp. 929–946, 2006.

[126] M. D. Bevan, J. F. Atherton, and J. Baufreton, "Cellular principles underlying normal and pathological activity in the subthalamic nucleus," *Curr. Opin. Neurobiol.*, vol. 16, pp. 621–628, 2006.

[127] D. Barraza, H. Kita, and C. J. Wilson, "Slow Spike Frequency Adaptation in Neurons of the Rat Subthalamic Nucleus," *J. Neurophysiol.*, vol. 102, pp. 3689–3697, 2009.

[128] C. J. Wilson, A. Weyrick, D. Terman, N. E. Hallworth, and M. D. Bevan, "A Model of Reverse Spike Frequency Adaptation and Repetitive Firing of Subthalamic Nucleus Neurons," *J. Neurophysiol.*, vol. 91, pp. 1963–1980, 2004.

[129] A. R. Aron, "The Neural Basis of Inhibition in Cognitive Control," *Neurosci.*, vol. 13, no. 3, pp. 214–228, 2007.

[130] S. Jahfari, K. R. Ridderinkhof, A. G. E. Collins, T. Knapen, L. J. Waldorp, and M. J. Frank, "Cross-Task Contributions of Frontobasal Ganglia Circuitry in Response Inhibition and Conflict-Induced Slowing," *Cereb. Cortex*, vol. 29, pp. 1969–1983, 2019.

[131] F.-E. François-Brosseau, K. Martinu, A. P. Strafella, M. Petrides, F. Simard, and O. Monchi, "Basal ganglia and frontal involvement in self-generated and externally-triggered finger movements in the dominant and non-dominant hand," *Eur. J. Neurosci.*, vol. 29, pp. 1277–1286, 2009.